List of Abstracts and Posters

Supergen ORE Hub: ECR Forum
5th November 2019

	Forename	Surname	University	Title
1	Mustafa	Abdelrahman	Hull	Control design for floating offshore wind turbines
2	Matthew	Allmark	Cardiff	CFD surface effects on flow conditions and tidal stream turbine performance
3	Abel	Arredondo Galeana	Edinburgh	Morphing blades for load alleviation of tidal turbines
4	Scott	Brown	Plymouth	Developing a Coupled CFD Model for Evaluating Floating Tidal Stream Concepts
5	James	Carroll	Strathclyde	Wind energy O&M research
6	Xiaosheng	Chen	Oxford	Multi-scale offshore wind farm modelling
7	Matteo	Ciantia	Dundee	Micromechanical modelling of jacked piles in sand
8	Charlotte	Cochrane	Edinburgh	Abstract: Assessing the economic benefit, technological innovation opportunity and ecological effects of the UK deployment of ORE technology Poster: Investigating the value to the UK economy of ocean energy: Scenarios to 2050
9	Kamyab	Givaki	Napier	Machine learning for power system impedance estimation
10	Siya	Jin	Plymouth	Numerical models of a floating hinged raft wave energy converter
11	Wei	Kang	Manchester	Near wake characteristics comparison of a tidal stream turbine with URANS-AL model
12	Katherine	Kwa	Southampton	Plate anchors for offshore floating facilities: soil-anchor-floating system interactions
13	Liang	Li	Strathclyde	Real-time wave energy control based on machine learning
14	Yibo	Liang	Strathclyde	Future offshore floating wind platform – challenge and opportunity
15	Lilian	Lieber	Queen’s Belfast	Development of novel low-cost methods to understand environmental processes in highly energetic ORE sites

16	Zi	Lin	Strathclyde	HOME-Offshore WP1.2 – Offshore wind turbine multi-physics modelling
17	Yanhua	Liu	Hull	Individual pitch actuator monitoring of offshore wind turbines
18	Saeid	Lotfian	Strathclyde	Programmable flexible materials for mooring and station keeping
19	Edward	Mackay	Exeter	Motion damping of floating offshore wind turbines using porous materials
20	Marinos	Manolesos	Swansea	Abstract: Aerodynamic and Aeroelastic Research at the new Swansea University Poster: Flow control for wind turbine airfoils
21	Pablo	Ouro	Cardiff	Wake structure of tidal stream turbine arrays under increasing flow depth
22	Alberto	Rabaneda	Hull	Datacube services for the offshore renewable energy industry in the UK
23	Edward	Ransley	Plymouth	The collaborative computational project in wave structure interaction (CCP-WSI)
24	Pal	Schmitt	Queen's Belfast	Assessing free surface effects in tidal turbine simulations
25	Shuo	Shi	Hull	Learning-based robust control for offshore wave energy converters
26	Dimitris Liang	Stagonas Yang	Cranfield	One-fluid formulation for floating offshore renewable energy devices
27	Neda	Trifonova	Aberdeen	Modelling spatial and temporal species dynamics in response to changes in climate and productivity in the North Sea
28	David	Wilkie	UCL	A risk assessment framework for offshore wind turbines

Control Design for Floating Offshore Wind Turbines

Mustafa Abdelrahman and James Gilbert
University of Hull, Hull, UK
m.Abdelrahman@hull.ac.uk, j.m.gilbert@hull.ac.uk

Introduction

Why go offshore?

- Onshore limitations: limited sites & visual/acoustic pollution.
- Stronger & consistent wind with less shear.
- Larger size Wind turbines can be constructed.

Fig. 1: Main categories of Floating Offshore Wind Turbines (FOWT)

What control does in FOWT system?

- Max. power in region 2. Regulation power and rotor speed in region 3
- Increase fatigue life by reducing structural loads.
- Stabilize FOWT platform.

Research Aim

- Develop **Reliable** and **low cost,** control systems to minimize fatigue and regulate turbine power and speed.

Research Plan

Task1: Literature Review
- Identify state of the art control methods for FOWT
- Specify limitations and research gaps

Task2: Simulation & Evaluation
- Build generic Control Design FOWT model in Matlab/Simulink , and validate using FAST.
- Compare control methods in terms of Performance, Reliability & Cost.

Task3: Novel ideas
- Investigate rejecting wave disturbance via Unknown Input Estimation (UIE) techniques.
- Investigate rationale of multi-objective control with extra actuator(s) installed on FOWT platform.

State of the Art FOWT control

FOWT Control category	SISO control loop(s): One or two PI/ PID loop(s) with gain scheduling.	Multi-Objective MIMO control: Advanced Model-based control used; H_∞, LQR, LQG, MPC & disturbance accommodating control (DAC).	Structural control: Extra actuator(s) added to the FOWT, e.g. Tuned Mass Damper(TMD), Tuned Liquid column Damper (TLCD) & Active Vertical-Vane
Pros.	• Simple: Small no. sensors • acceptable station-keeping and some load-reduction • Robustness	• Better performance than SISO control: o Power & Speed fluctuation reduction. o Tower Fatigue (Loads) Reduction	• Stabilizing platform & reduce tower fatigues • No interference with power & speed regulation
Cons.	• Power and speed fluctuations increase • Fatigues still higher than land-based turbines	• Many Sensors required, robustness and sensor faults become issue • increased blade pitch rate (fatigue!) • Compromise control objects needed (e.g. generator efficiency and platform stability)	• Extra cost & consume some power. • Increased Mass and Stroke (TMD) • Changes in platform dynamics & design (TLCD)
Examples	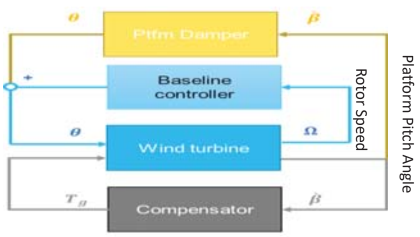 A simple PI controls for FOWT [5]	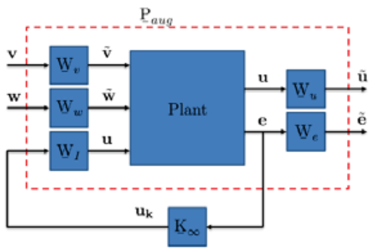 Advanced H_∞ FOWT control [3]	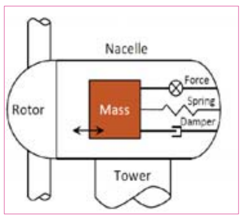 TMD [1] 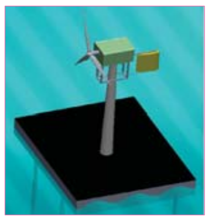 Active Vertical –Vane [1] 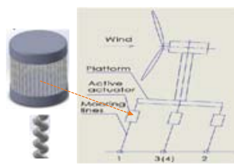 STAM* [4] 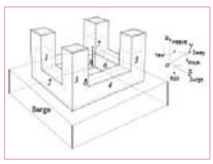 BTLCD [2]

* thermally–actuated sewing thread artificial muscle

References

[1] Jalili, Kaveh, Yaoyu Li, and Mario A. Rotea. "Pitch and roll motion control of a floating wind turbine with hybrid actuation." *ASME 2014 Dynamic Systems and Control Conference*. American Society of Mechanical Engineers, 2014.

[2] Tong, Xin, Xiaowei Zhao, and Aris Karcanias. "Passive vibration control of an offshore floating hydrostatic wind turbine model." *Wind Energy* 21.9 (2018): 697-714.

[3] Ho mer, Jeffrey R. *Physics-based control-oriented modelling for floating offshore wind turbines*. Diss. University of British Columbia, 2015.

[4] Li, Yaoyu, and Zhongyou Wu. "Stabilization of floating offshore wind turbines by artificial muscle based active mooring line force control." *2016 American Control Conference (ACC)*. IEEE, 2016.

[5] Yu, Wei, et al. "Evaluation of control methods for floating offshore wind turbines." *Journal of Physics: Conference Series*. Vol. 1104. No. 1. IOP Publishing, 2018.

CFD surface effects on flow conditions and tidal stream turbine performance

Catherine Lloyd*, Matthew Allmark, Robert Ellis, Stephanie Ordonez, Allan Mason-Jones, Cameron Johnstone, Tim O'Doherty, Gregory Germain and Benoit Gaurier
*Cardiff Marine Energy Research Group (CMERG), School of Engineering, Cardiff University, Cardiff, Wales, UK

NUMERICAL MODELLING

A 'free surface' and a 'free slip' numerical model were created, to assess the differences between their surface boundary conditions and how this causes changes in the generated flow conditions and turbine performance under uniform current flow conditions. The 'free slip' model was a single-phase, incompressible flow model with the 'top' boundary at the still water level using the 'free slip' boundary condition. The 'free surface' model was a homogenous, multiphase model with a distinct free surface interface between the water and air phases. The 'top' boundary was in the air region of the model and specified as an 'opening' allowing bidirectional flow across the boundary. Development of the model was split into 3 mains sections: **Geometry, Mesh** & **Physics setup.**

GEOMETRY

The model geometry and mesh generation were developed using ANSYS CFX 18.0. Figure 1 shows the dimensions of the geometry for each model type. The height of the domain in the 'free surface' model was 2.86m as space was required for both water and air, so an air space of 0.86m was added above the 2m water depth. The 'free slip' model was single fluid flow only and therefore the height of the domain was the same as the depth of the water (2m).

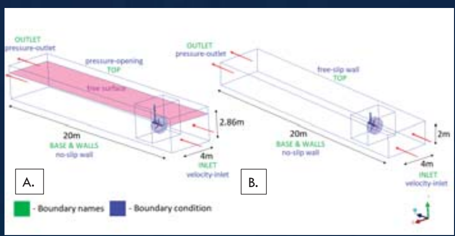

Figure 1. Geometry development and boundary conditions imposed for: (a) 'free surface' and; (b) 'free slip' model.

MESH

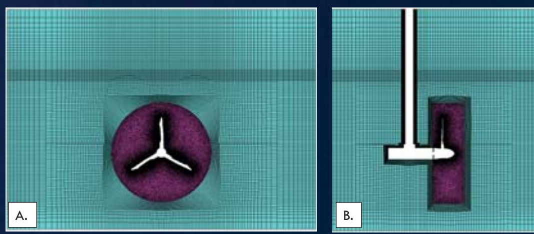

Figure 2. Final mesh for the 'free surface' model, viewed from the: (a) front and; (b) side.

The mesh was generated using a mixture of 'hexa' and 'tetra' meshing, as described by [1], with the final mesh for the 'free surface' model shown in Figure 2. The 'free slip' mesh was identical but with the mesh for the 'air' region removed.

PHYSICS SETUP

The simulations were set up as a transient analysis using a uniform current flow of 1.01 m/s. The rotating part of the turbine was enclosed in a cylindrical subdomain to allow the Multiple Frames of Reference (MFR) technique to be used. This method allows the subdomain to rotate around a given axis at a specified angular velocity, simulating the turbine rotation. The angular velocity of the turbine was set to test Tip Speed Ratios (TSR) between 0-7. The SST turbulence model was used to close the Reynolds Averaged Navier Stokes (RANS) equations in order to resolve the flow conditions. The boundary conditions used in both models were set as shown in Figure 1 and are detailed in Table 1.

Table 1. A summary of the boundary conditions used in the numerical models.

Boundary	Boundary condition: 'free surface' model	Boundary condition: 'free slip' model
inlet	Velocity-inlet $\bar{W} = 1.01\ m/s$	Velocity-inlet $\bar{W} = 1.01\ m/s$
outlet	Pressure-outlet $P_{ref} = (\rho_{water} - \rho_{air}) \cdot g \cdot (h - y)$	Pressure-outlet $P_{ref} = 0\ Pa$
top	Pressure-opening Entrainment with opening pressure: $P_{rel} = 0\ Pa$	Free-slip wall
base	No-slip wall	No-slip wall
walls	No-slip wall	No-slip wall

EXPERIMENTAL TESTING

The 2 different numerical models were compared to experimental data obtained at IFREMER, Boulogne-Sur-Mer, France [2]. The new turbine is a development of a previous Cardiff University design [3]. It is a 3 bladed horizontal axis tidal turbine of approximately 1:20 scale and has a diameter of 0.9m.

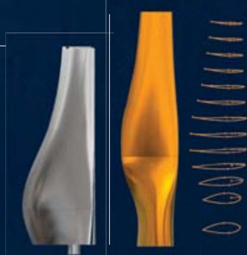

OLD NEW

- Blade profile: Wortmann FX63-137
- Blade length = 0.383m
- Blade twist = 19 °
- Pitch angle = 8 °
- Diameter = 0.9m
- Blade length = 0.383m

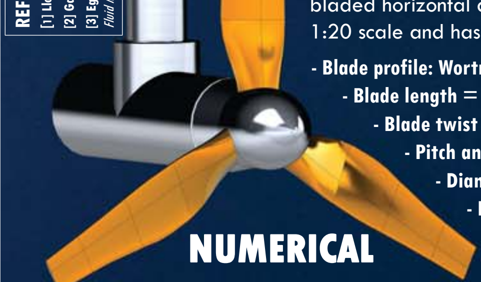

NUMERICAL MODEL COMPARISON

The non-dimensional coefficient of power (C_p) and coefficient of thrust (C_t) were compared between data sets. Figure 4 shows that the numerical results for C_p and C_t have good agreement with the experimental data for TSR ≤ 5, after which the numerical results drop off a lot quicker than the equivalent experimental values.

As the angular velocity increases, the flow conditions become more complex and it is possible that flow separation is occurring in a less refined part of the mesh. This suggests the need for different meshes depending on the TSR being investigated and therefore this study investigates models at a TSR of 3-5. These TSRs were of interest as it is the region around peak power and this region gave the best agreement with experimental data.

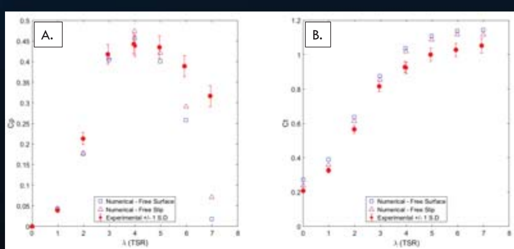

Figure 4. Comparison of numerical and experimental data for: (a) C_p and; (b) C_t.

The average performance characteristics show little difference between the numerical models. Therefore, the transient dynamic loadings were investigated (Figure 3). The main findings were:

- There was little difference in average individual blade torque and thrust between the models.
- The 'free surface' model estimated the average thrust on the hub to be over double that of the 'free slip' model, giving 20.1 N and 8.2 N respectively. This is due to the addition of hydrostatic forces in the 'free surface' model which affect the hub significantly.
- The fluctuation of the individual blade thrust results show good agreement between the 2 model types.

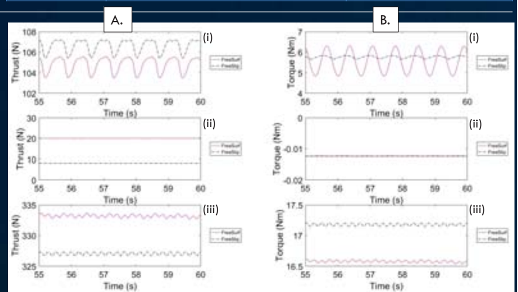

Figure 3. 'Free surface' and 'free slip' model results, for (a) thrust and (b) torque at TSR 4 relating to: (i) blade 1, (ii) the hub and; (iii) the turbine total (all blades and hub).

- The fluctuation of the individual blade torque results for the 'free surface' and 'free slip' models are 0.77 Nm and 0.06 Nm respectively. Buoyancy forces present in the 'free surface' model contribute to the blade torque when they are horizontal in the water column but not when they are vertical. This results in the oscillations seen in the torque results for each blade.
- The total turbine torque fluctuation is the same for the 2 model types. Each turbine blade is 120° out of phase and so each blade cancels the others out and reduces the amplitude of the overall frequency. Therefore, if only the total turbine torque was investigated, these substantial fluctuations in the blade torque would be overlooked and potential design considerations for the turbine blades ignored. This could be crucial in fatigue analysis and survivability of the tidal device.

REFERENCES:

[1] **Lloyd et al. 2018.** Development of a Wave-Current Numerical Model using Stokes 2nd Order Theory. *Proceedings of the 4th AWTEC.* Taipei, Taiwan; 9th -13th Sept 2018.

[2] **Gaurier et al. 2013.** Flume tank characterization of marine current turbine blade behaviour under current and wave loading. *Renewable Energy; vol. 59, pp. 1-12, 2013.*

[3] **Egarr et al. 2004.** Feasibility study using computational fluid dynamics for the use of a turbine for extracting energy from the tide. *Proceedings of the 15th Australasian Fluid Mechanics Conference.* University of Sydney; Australia, 13-17 December 2004.

MORPHING BLADES FOR LOAD ALLEVIATION OF TIDAL TURBINES

Dr Abel Arredondo-Galeana[a], Dr Anna Young[b], Dr Ignazio Maria Viola[a]

[a] Institute for Energy Systems, School of Engineering, University of Edinburgh

[b] Department of Mechanical Engineering, University of Bath

Motivation

The use of passive unsteady load mitigation technology for wind and tidal turbines, such as bend-twist coupling, is typically limited to low frequency fluctuations and is not suitable to large blades, due to structural rigidity requirements.

Active control systems, such as actuated flaps, can respond to higher frequencies than whole-blade passive devices due to their smaller size. However, active systems may reduce turbine reliability. Hence there is a need to develop a high-frequency passive technology if turbines are to survive in the harsh marine environment.

We have shown analytically and with CFD that the unsteady loads on a turbine can be completely cancelled with a chordwise flexible blade. Additionally, the model shows that when the blade is rigid apart from a portion near the trailing edge, the unsteady load mitigation is proportional to the length of the flexible portion compared to the blade chord.

Passive morphing mechanism

The effectiveness of the morphing blade concept was demonstrated by testing a foil equipped with a flap where a constant pitch moment is applied. When the flow is stationary, the buoyancy force causes the flap to deflect upwards, but when the flow is moving, the buoyancy is balanced by the hydrodynamic force and the flap is aligned with the blade (Figure 1).

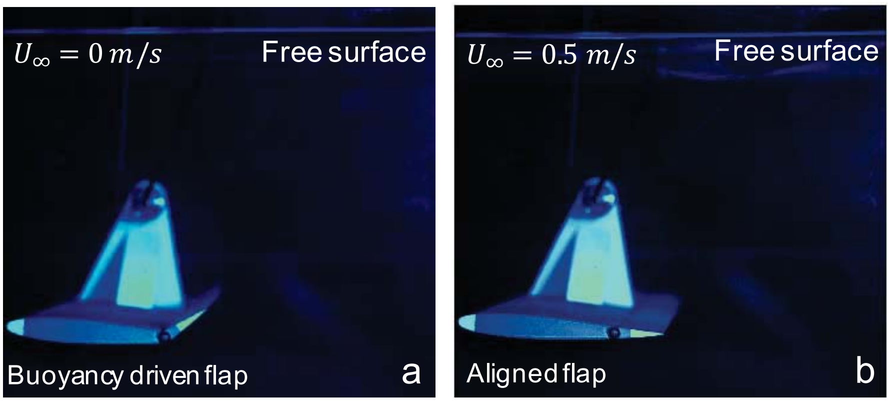

Figure1– a) Morphing blade in a water flume with stationary flow, and b) with moving flow

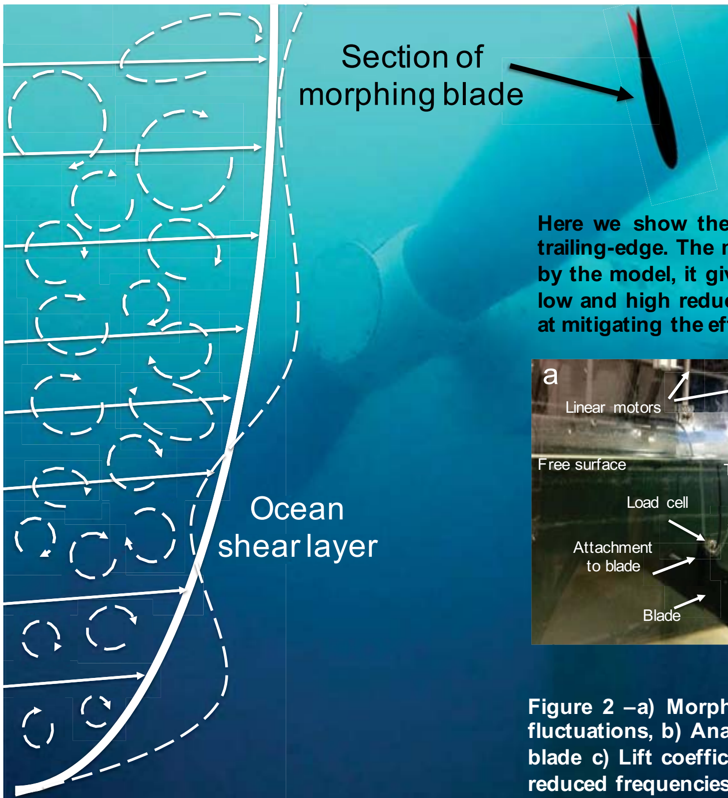

Methodology and results

Here we show the experimental validation of the model with a blade that has a morphing trailing-edge. The morphing trailing-edge extends 25% of the chord of the blade, as predicted by the model, it gives a 25% reduction in unsteady load. The mechanism has been tested at low and high reduced frequencies to demonstrate the effectiveness of the morphing concept at mitigating the effect of a range of gusts.

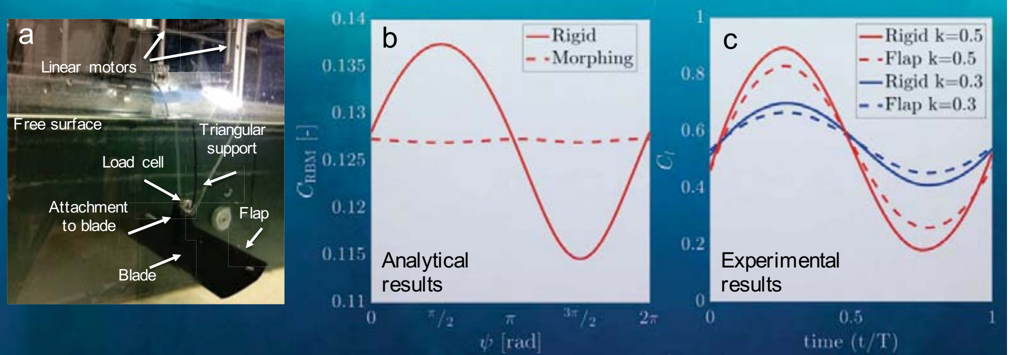

Figure 2 –a) Morphing blade prototype mounted on a heaving rig modelling unsteady flow fluctuations, b) Analytically computed root bending moment of a rigid and chordwise flexible blade c) Lift coefficients for a blade prototype tested at $\alpha = 5°$ with and without flap, at two reduced frequencies, k=0.1, 0.3 (blue, red).

References

1. Tully, S. and Viola, I.M. (2016), "Reducing the wave induced loading of tidal turbine blades through the use of a flexible blade", ISROMAC 2016, 10-15 April, Honolulu, USA, p. 9.
2. Young, A.M., Farman J.R., Miller Robert J. (2016), "Load alleviation technology for extending life in tidal turbines", RENEW 2016, 4-26 October, Lisbon, Portugal, p.521-530
3. Scarlett, G.T., Sellar, B., van den Bremer, T., Viola, I.M. (2019), "Unsteady hydrodynamics of a full-scale tidal turbine operating in large wave conditions", Renewable Energy, p.199-213
4. Sequeira C.L. and Miller R. J. (2014) "Unsteady Gust Response of Tidal Stream Turbines", Oceans - St. John's, IEEE, pp. 1–10.
5. Pisetta, G., Viola, I.M. (2020), "Passive load control of a tidal turbine", Renewable Energy [submitted].

THE UNIVERSITY of EDINBURGH

NOVA INNOVATION

UNIVERSITY OF BATH

Developing a Coupled CFD Model for Evaluating Floating Tidal Stream Concepts

Scott Brown*[1], Edward Ransley[1], Deborah Greaves[1], Eamon Guerrini[2]

*scott.brown@plymouth.ac.uk, [1]University of Plymouth, [2]Modular Tide Generators Ltd.

CCP-WSI
a Collaborative Computational Project in Wave Structure Interaction

Introduction

Floating devices have the potential to unlock unobtainable parts of the tidal stream energy resource, however; the proximity of the free surface raises concerns over both the power delivery and the survivability of these systems. Therefore, the aim of this study is to ***develop** an **open-source**, **efficient** and **sustainable, numerical tool** for assessing the **complete** floating tidal stream system in **real conditions.*** The present work describes the development process for the model, and focuses on ongoing validation against physical data for the Modular Tide Generators (MTG) floating tidal stream concept, which is a catamaran-style platform with a submerged, horizontal-axis tidal turbine (HATT) and a four-point catenary mooring system (Figure 1).

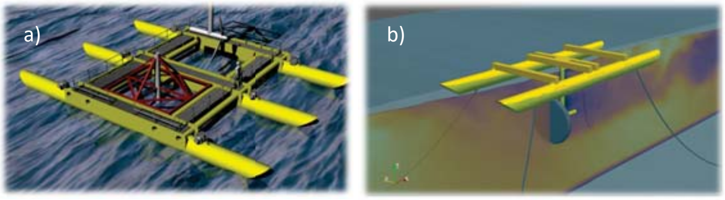

Figure 1: *The MTG platform concept: a) Render of the 3-hull platform; b) Numerical simulation of the 2-hull platform including the moorings; turbine region; and turbine effect on the fluid.*

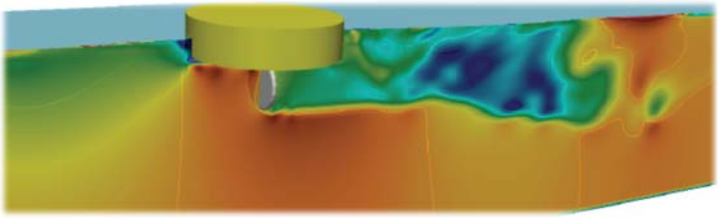

Figure 2: *Visualisation of the numerical output for a generic platform in wave-current conditions.*

Numerical Model

The numerical model uses a fully-nonlinear, coupled approach, based on the open-source CFD libraries of OpenFOAM and consists of five key components:

- **The hydrodynamic model** [1] solves the Reynolds-Averaged Navier-Stokes (RANS) equations for two, incompressible, isothermal and immiscible fluids, with the interface tracked via an algebraic volume of fluid (VoF) advection scheme.
- **Wave generation/absorption** is achieved via expression-based boundary conditions assisted by the relaxation zone technique provided by the waves2Foam toolbox [2].
- **The turbine model** [3] is based on a weighted body force implementation. In short, the model identifies the instantaneous position of the turbine region; estimates the thrust on the turbine using actuator theory based on the local flow velocity; applies this force in the equation of motion; and adds an additional, equal and opposite force to the hydrodynamic model to achieve two-way coupling (Figure 2).
- **The moorings** are expressed as an additional force in the equation of motion of the body. At each time step, the force from each mooring line, is calculated using the static catenary formulation [4].
- **The rigid body solver** uses a deforming mesh technique to track the instantaneous position of the floating platform in six degrees of freedom. This solver takes into account any effects caused by the additional forces from the turbine and mooring by including additional accelerations in the equation of motion.

Full System Validation

<u>Physical Modelling:</u> To provide validation data for an entire floating tidal stream system, physical experiments were conducted in the COAST Laboratory at the University of Plymouth, UK. A 1:12 scale model of the MTG concept was constructed with the submerged HATT being approximated using a porous disc (Figure 3). The program consisted of a series of fixed tests, where the model was fixed to the gantry above the basin via a 6-axis load cell, and moored tests, where the model was floating and restrained by catenary mooring chains. A wide range of regular and irregular wave tests were conducted, for both set-ups, in combination with a range of current conditions and both with and without the turbine loaded, allowing for an incremental comparison.

<u>Preliminary Observations:</u> The numerical model captures the motion of the platform; non-linearities in heave; the offsets in surge caused by the presence of the turbine; and increase in the mean total mooring load. It also captures an increase in maximum turbine load when the device is moored rather than fixed, as seen in the physical data. This is a key observation for floating tidal platforms due to the implications on both turbine fatigue and power delivery, and could influence future design of the moorings.

<u>Ongoing Work:</u> The thrust amplitude response is consistently under-estimated in wave-only conditions, likely due to actuator theory not being ideally suited for non-uniform reversing flow conditions. Therefore, the turbine model will be modified to incorporate an improved dynamic response formulation, as well as improved physics such as: radial weighting; rotational effects; and tip corrections. The mooring load response also differs substantially from the physical data, and hence, to improve reproduction, future work will focus on including a dynamic catenary formulation and drag on the mooring lines.

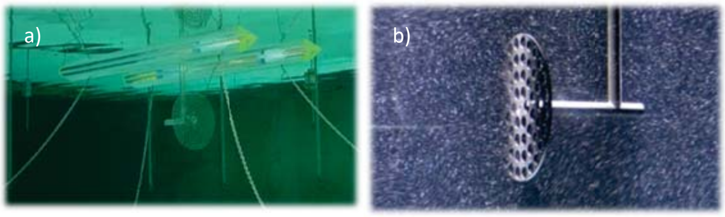

Figure 3: *Photographs from the COAST Laboratory experiments: a) Underwater view of the full 1:12 scale model in the Ocean Basin; b) Calibrating a porous disc using PIV in a wave flume.*

Turbine Model Verification and Validation

An incremental approach has been utilised to validate the numerical model, where each component of the system has been isolated and systematically tested to ensure it is both accurate and robust. In particular, the turbine model has been verified against theoretical solutions based on actuator theory, and has been evaluated for sensitivity to key parameters such as flow speed; thrust coefficient; mesh resolution; mesh alignment; and accuracy under prescribed motion (a crucial consideration when coupled with the rigid body solver) [3]. Furthermore, the effect on the hydrodynamics has been validated (Figure 4 [3]) against experimental data for a porous disc in a steady current [5]. The results showed that the velocity deficit profile was predicted accurately [3], but further work is required to better capture the turbulent kinetic energy profile.

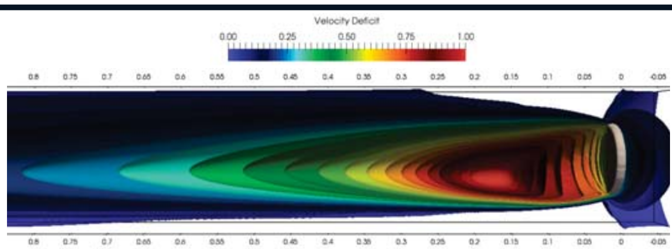

Figure 4: *Numerical prediction of velocity deficit behind an actuator disc model. [3]*

References

[1] Rusche, H. (2002). “Computational fluid dynamics of dispersed two-phase flows at high phase fractions” *Ph.D. Thesis,* Imperial College of Science, Technology & Medicine.

[2] Jacobsen, N., Fuhrman, D., Fredsøe, J. (2012). “A wave generation toolbox for the open-source CFD library: OpenFOAM”, *Int. J. Num. Methods in Fluids* 70, 1073–1088.

[3] Brown, S., Ransley, E., Greaves, D. (2020). “Developing a coupled turbine thrust methodology for floating tidal stream concepts: verification under prescribed motion”, *Renewable Energy* 147, 529-540.

[4] Bruinsma, N., Paulsen, B., Jacobsen, N. (2018). “Validation and application of a fully nonlinear numerical wave tank for simulating floating offshore wind turbines”, *Ocean Eng.* 147, 647–658.

[5] Myers, L., Bahaj, A. (2010) “Experimental analysis of the flow field around horizontal axis tidal turbines by use of scale mesh disk rotor simulators”, *Ocean Eng.* 37, 218-227.

Acknowledgements

This work was funded as part of Innovate UK Projects 102217 and 103499 via the Industrial Strategy Fund. The code presented here is available through the Collaborative Computational Project in Wave Structure Interaction (CCP-WSI) [EP/M022382/1], which aims to bring together the community of researchers, data, code and expertise in the area of wave structure interaction (https://www.ccp-wsi.ac.uk).

MODULAR TIDE GENERATORS LIMITED

UNIVERSITY OF PLYMOUTH School of Engineering, Computing & Mathematics

UNIVERSITY OF EXETER

Innovate UK Technology Strategy Board

Supergen Offshore Renewable Energy

Wind Energy O&M Research

ECR Name: James Carroll

Lecturer and Chancellor's Fellow
University of Strathclyde, Glasgow, Scotland.
j.carroll@strath.ac.uk

University of Strathclyde Engineering

Wind Turbine Component Failure and Remaining Useful Life Prediction

1. Team led by James Carroll in Turbine Component Failure and RUL prediction:

Wind turbine Expertise

Signal Processing Expertise

Machine learning expertise

Wind turbine component failure and RUL prediction

Sofia Koukoura	Alan Turnbull	Becky Corley	Conor McKinnon	Dr David Ferguson
Gearbox Failure and RUL Prediction (Temperature and vibration data)	Generator Failure and RUL Prediction (Temperature and vibration data)	Gearbox Failure Prediction (Thermal Modelling)	Gearbox Failure Prediction (Oil Analysis) Pitch failure prediction	Industry Knowledge Exchange with Turner Iceni

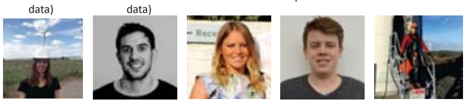

Gearbox failure prediction. PhD Student: Sofia Koukoura

Gearbox Failure and RUL Prediction (Temperature and vibration data)

Example of Sofia's work: Gearbox IS tooth issue.

Feature Extraction:

1. Side band analysis
   - Sideband energy ratio
   - Sideband average power
   - Sideband Modulation Lifting Factor
2. Cepstrum Analysis
3. Time Synchronous Averaging
4. Amplitude Modulation
5. Empirical Mode Decomposition
6. Spectral Kurtosis
7. Combination of sideband Cepstrum and AM

Classifiers:

1. Decision Tress
2. KNN
3. SVMs
4. ANN

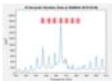

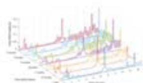

Findings to date:

- Different Classifiers perform better depending on features used
- Best performing combination is Sideband analysis with SVM
- 3 features combined (SBA, Cepstrum and AM) led to overall best performance with SVMs

Generator failure prediction. PhD Student: Alan Turnbull

Generator Failure and RUL Prediction (Temperature and vibration data)

Example of Alan's work: DFIG bearing looseness issue

15 identical wind turbines across 7 wind farms exhibiting same failure mode.
K-nearest neighbour

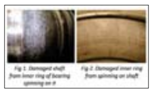

Results:

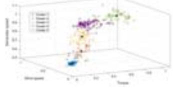

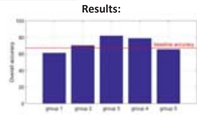

Turbine Reliability and O&M cost Modelling

Offshore Failure Rates of Wind Turbines and Their Subassemblies

- From Offshore 8 Wind Farms located throughout Europe
- Split into Minor Repair, Major Repair and Major Replacement
- Pitch system has the higest toal failure rate. Gearbox has the highest major replacement failure rate.

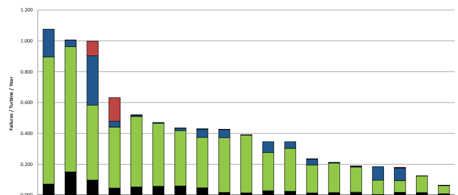

	Pitch / Hyd	Other Components	Generator	Gearbox	Blades	Grease / Oil / Cooling Liq.	Electrical Components	Contactor / Circuit Breaker / Relay	Controls	Safety	Sensors	Pumps/ Motors	Hub	Heaters / Coolers	Yaw System	Tower / Foundation	Power Supply / Converter	Service Items	Transformer
Major Replacement	0.001	0.001	0.095	0.154	0.001	0.000	0.002	0.002	0.001	0.000	0.000	0.000	0.001	0.000	0.001	0.000	0.005	0.000	0.001
Major Repair	0.179	0.042	0.321	0.038	0.010	0.006	0.016	0.054	0.054	0.004	0.070	0.043	0.038	0.007	0.006	0.089	0.081	0.001	0.003
Minor Repair	0.824	0.812	0.485	0.395	0.456	0.407	0.358	0.326	0.355	0.373	0.247	0.278	0.182	0.190	0.162	0.092	0.076	0.108	0.052
No Cost Data	0.072	0.150	0.098	0.046	0.053	0.058	0.059	0.048	0.018	0.015	0.029	0.025	0.014	0.016	0.020	0.004	0.018	0.016	0.009

Comparison of failure rates between turbine types

- Over 1800 DFIGs over 5 years (3391 Turbine Years of Data)
- 400 PMG FRCs over 3 years (511 Turbine Years of Data)
- Same turbine type different (Mk version so same turbine except for drivetrain)

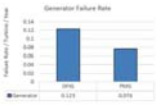

Failure rates combined for over all configuration failure rate

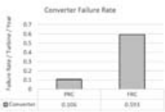

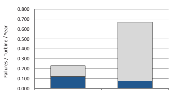

	DFIG	PMG
Converter	0.106	0.593
Generator	0.123	0.076

- % difference between generator and convertors onshore applied to offshore data on previous slide.
- 3 stage Gearbox and "Rest of Turbine" Failure Rate assumed the same

O&M Costs for Different Wind Turbine Types

- O&M costs at 50km ~45% lost production, 45% transport costs, 5% staff and 5% repair costs
- Jump in lost production costs at 100km related to availability

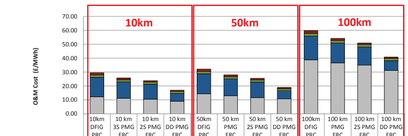

	10km DFIG PRC	10 km 3S PMG FRC	10 km 2S PMG FRC	10 km DD PMG FRC	50km DFIG PRC	50 km PMG FRC	50 km 2S PMG FRC	50 km DD PMG FRC	100km DFIG PRC	100 km PMG FRC	100 km 2S PMG FRC	100 km DD PMG FRC
Repair Costs (£)	1.61	1.26	0.94	0.79	1.65	1.26	1.15	0.80	1.88	1.46	1.08	0.89
Staff Costs (£)	1.71	1.63	1.6	1.49	1.74	1.65	1.65	1.5	2.01	1.9	1.85	1.71
Transport Costs (£)	13.95	11.75	10.73	5.66	14.37	12.05	11.06	5.88	17.03	14.24	13	7.02
Lost Production Costs (£)	12.26	11.16	10.53	9.04	14.37	13.03	11.68	10.72	38.81	36.63	35	31.13

Reducing downtime and Improving availability/O&M costs:

- 3 stage DFIG PRC: Decrease failure rate in DFIG
- DD and 2 stage PMG FRC focus on the converter
- 3 stage PMG, focus on gearbox up to 50km and converter at 100km

X-Rotor Development and X-Rotor O&M cost Modelling

The X-Rotor Offshore Wind Turbine Concept

- Primary rotor rotates on the vertical axis
- No power take off on vertical axis
- High speed horizontal axis secondary rotors
- No requirement for gearbox or multi-pole generator
- X-Shape reduces overturning moments
- Reduced requirement for Jack up vessel and reduced failure rates

X-Rotor Benefits

1. Cost of energy reduction (Lower capital costs and lower O&M costs)
2. Floating platform potential (lower centre of gravity compared to traditional HAWT)
3. Up-scaling potential (Additional blades and secondary rotor)

X-Rotor O&M Cost Investigation

- X-Rotor O&M costs compared to 4 different turbine types
- Strathclyde O&M cost model used
- Model and model inputs adjusted to represent the X-Rotor
- O&M costs from existing turbines come from a published paper
- Same methodology and hypothetical site used for like for like comparison with results

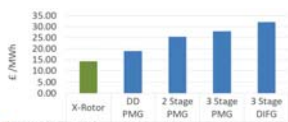

	X-Rotor	DD PMG	2 Stage PMG	3 Stage PMG	3 Stage DFIG
O&M Costs	14.35	18.90	25.54	27.99	32.13

- X-Rotor O&M costs 43% lower than the average O&M cost for four existing turbine types
- No gearbox or multipole generator failures.
- Greatly reduced requirement for Jack-up vessel.

Multi-Scale Offshore Wind Farm Modelling

Xiaosheng Chen, Christopher Vogel, Richard Willden
Department of Engineering Science, University of Oxford
Xiaosheng.chen@eng.ox.ac.uk

Wind Turbine Wake Effects in Large Wind Farms

Evidence from the Field

- Field data shows conditions experienced by a turbine in a large farm are dependent on the incident flow direction and arrangement of upstream and neighbouring turbines.
- Downstream turbine performance affected by wakes and turbulence of upstream turbines.
- Limitations of turbine farm models are due in part to overly simplified single wake models and non-physical wake interaction modelling.
- Poor lifetime yield prediction, and poor unsteady loading and fatigue damage rate prediction as a result of low fidelity wake evolution and interaction modelling.

Source: Gunn (2018) in Scroby Sands, UK

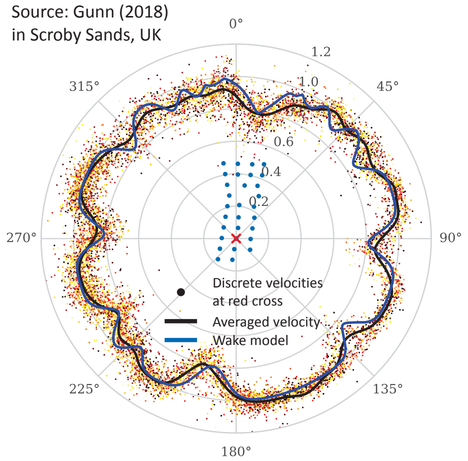

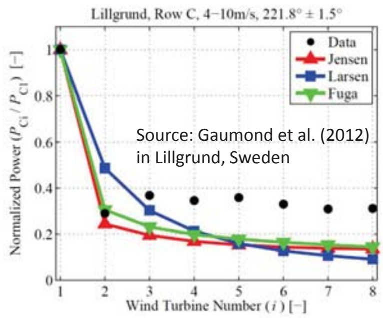

Source: Gaumond et al. (2012) in Lillgrund, Sweden

Wake Evolution and Combination

Wake Interaction Scenarios

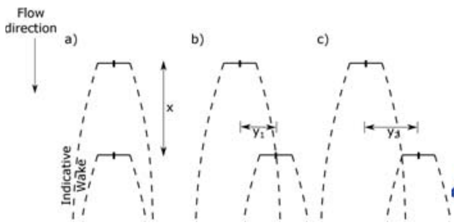

Source: Vogel & Willden (2019)

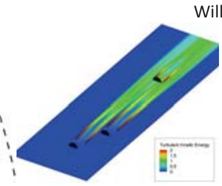

- Wake interactions in large wind farms occur for various turbine layouts.
- Performance of current wake superposition models are configuration dependant.
- Reduce-order modelling with embedded wake physics will improve wind farm prediction.

Wake Model Comparison

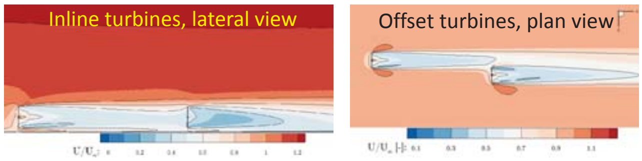

Predicted wake via superposition, 16 diameters downstream

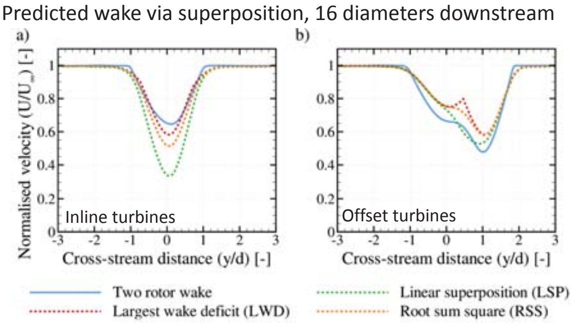

Wind Turbine Wake Modelling

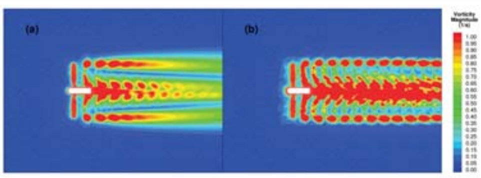

Source: Schluntz & Willden (2015)

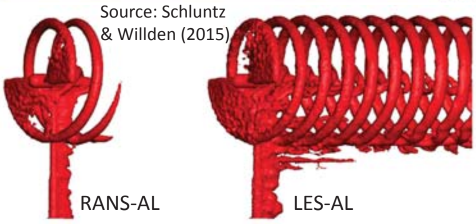

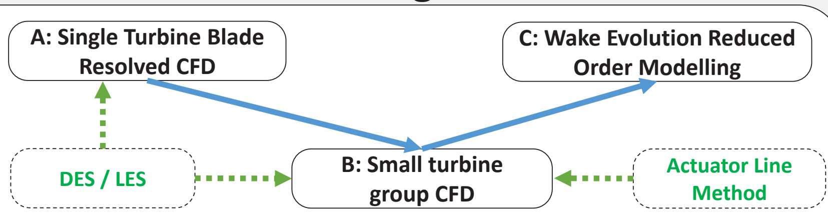

- Blade flows and wake structures by blade resolved CFD for large (10MW+) single wind turbines.
- Small (2-4) turbine group CFD investigation of wake interactions and merger with LES-AL for key turbine arrangements.
- Development of reduced-order wake evolution model based on simplified wake evolution & interaction theory, including turbulence transport.

References

- Gunn, K., 2018, Improvements to the eddy viscosity wind turbine wake model, *WindEurope Conference*.
- Gaumond et al., 2012, Benchmarking of wind turbine wake models in large offshore windfarms, *The science of Making Torque from Wind 2012*.
- Vogel and Willden, 2019, Investigation of wind turbine wake superposition models using RANS, *Wind Energy*.
- Schluntz and Willden, 2015, An actuator line method with novel blade flow field coupling based on potential flow equivalence, *Wind Energy*.

Acknowledgement

This project is funded as part of the SUPERGEN ORE Hub through EPSRC grant No. EP/S000747/1. The authors would like to thank the SUPERGEN ORE Hub and EPSRC for their support.

Micromechanical modelling of jacked piles in sands

Matteo O. Ciantia - University of Dundee, School of Science and Engineering, Dundee, UK
m.o.ciantia@dundee.ac.uk @MatteoCiantia

Introduction

A three-dimensional discrete element model is used to investigate the effect of grain crushing on the tip resistance measured by instrumented piles in a calibration chamber. The particles of the discrete model have a size-dependent crushing resistance whose material parameters were calibrated against an oedometer test and single grain crushing experiments, with additional validation by element tests. The numerical pile penetration tests agree encouragingly well with the instrumented pile experiments.

DEM crushing model

The pile simulations used the DEM crushable soil model proposed by Ciantia *et al*. (2015). The limiting crushing criterion considers the particle contact forces and the elastic stress induced within the spherical particles. Once this limit is reached, the particles split into smaller spheres (Figure1). Ciantia *et al*. (2015) showed that crushing to a 14-sphere final configuration gives a good match to macroscopic behaviour. This model is framed to be scalable and the same macroscopic response is obtained when the particle dimension is scaled by a factor, N, reducing the number of particles and hence computational costs.

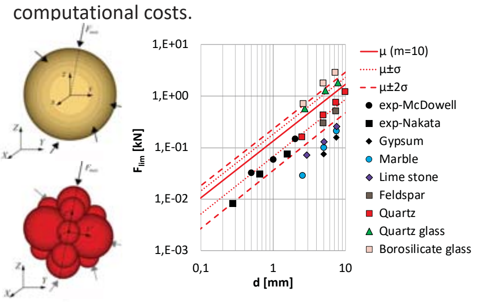

Figure 1. Particle limit contact force as a function of particle diameter, where $F_{lim} = \sigma_{lim,0}(d/Nd_0)^{-3/m}A$. Also shown are single grain crushing experiments by Yashima et al. (1987), Nakata et al. (2001) and McDowell (2002) after Ciantia et al. (2019).

Reproducing NE34 sand behaviour with DEM

The frictional and stiffness contact law parameters were calibrated by simulating drained triaxial compression of dense and loose specimens of NE34 sand (Figure 2a). The particle failure criterion parameters were calibrated simulating single particle crushing tests. Model validation was done simulating high pressure 1D compression tests (Figure 2b,c).

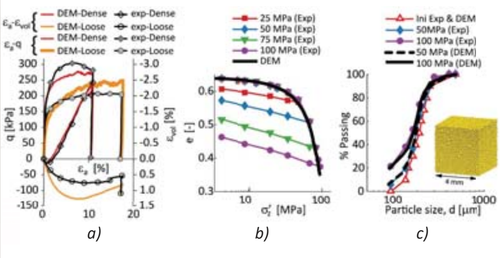

Figure 2. Contact model calibration: a) DEM simulation of drained triaxial compression test (cell pressure 100 kPa; experimental data from Seif El Dine et al., 2010). Crushing model validation by DEM simulation of oedometer tests in terms of b) effective vertical stress vs void ratio and c) PSD evolution.

Pile driving

The DEM procedures described by Ciantia et al. (2016) were applied to represent the conditions employed by Yang et al. (2010), in their Calibration Chamber (CC) model pile experiments. To make the simulations tractable, the particle dimensions were scaled by a factor of 39 and a reduced diameter chamber was adopted that contained ≈ 400,000 particles. Figure 3 shows good agreement between the CC pile tip resistance-penetration curves and the DEM (crushable) predictions for both the monotonic and cyclic jacking case.

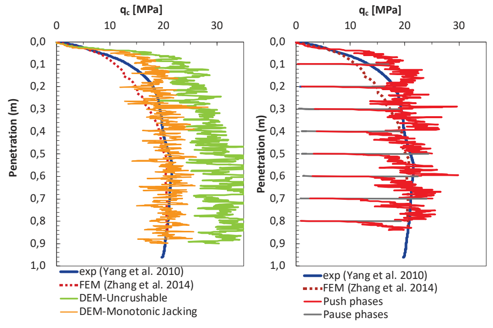

Figure 3. a) End-bearing capacity q_c versus penetration: Comparison between FEM (Zhang et al., 2014) (steady state qc = 21 MPa) and experimental results (Yang et al., 2010) and a) monotonic DEM and b) cyclic pile jacking DEM model.

Stress distributions

As detailed in Ciantia *et al*. (2019) particle DEM data at the end of each push and pause (unload) period can be used to determine the stresses within any portion of the model domain. The DEM model gave information on the sand stress regime generated by pile penetration, which match the experimental and FEM results (Figure 5). Figure 6 considers the decay of the radial stresses with increasing r/R during the push phases of penetration. These values are established at h/R=0.5 at three penetration stages and compared with experimental and FEM results.

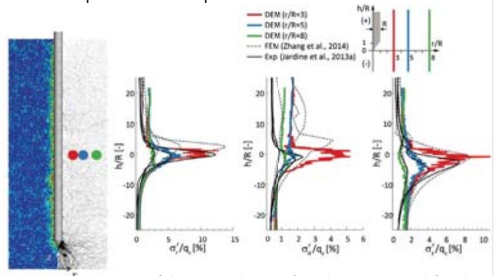

Figure 5. DEM, FEM (Zhang et al., 2014) and experimental (Jardine et al., 2013) comparison of stresses developed as pile tip advances. The radial circumferential and vertical stresses are normalized by q_c and refer to lines having at a distance r/R=3, 5 and 8 from the pile axis as sketched in the legend and on the image on the left.

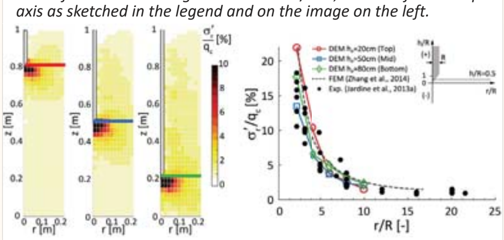

Figure 6. DEM, FEM (Zhang et al., 2014) and experimental (Jardine et al., 2013) comparison of normalized radial effective stress evolutions along the radial axis at h=0.5R above the tip.

The spatial variations of radial stresses around the shaft for the 'push' (penetrating) and 'pause' (unloaded) conditions are presented in Figure 7. The numerical predictions are in broadly good agreement with the experimental contour plots given by Jardine et al. (2013).

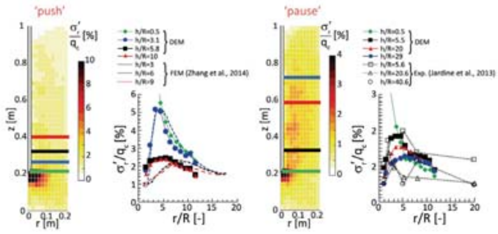

Figure 7. DEM radial stresses acting above pile tip during: (left) steady penetration and (right) (un-loaded) pause conditions. Where possible FEM and experimental results are also shown.

Discussion

Comparisons between DEM simulations performed with and without particle breakage highlights the impact of grain crushing on the stress relaxation experienced around the shaft. Parts (a), (b) and (c) of Figure 8 compare the stress profiles from analyses with crushable and unbreakable grains at h/R=7.5 above the tip, considering a zero-load pause period jacking stage of a cycle. Crushing accentuates the unloading close to the shaft and promotes the arching action. The arching developed around the shaft is clearly visible in parts (d) and (e) of Figure 8 where the contact force network and particles stress data are also represented.

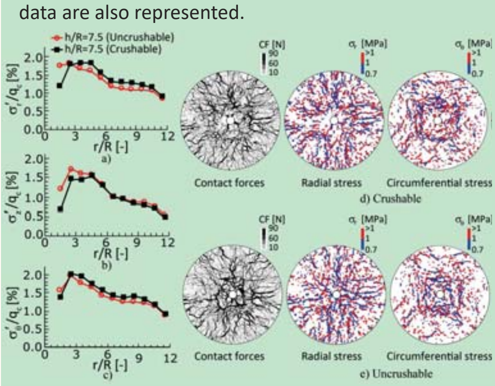

Figure 8. Radial profiles of (a) radial, (b) circumferential and (c) vertical stresses acting at h/R=7.5, comparing crushable and uncrushable simulations of the (unloaded) pause phases and demonstrating arching around the pile shaft: d) Uncrushable e) Crushable. Only particles with circumferential, radial and vertical stress>0.7MPa are shown: blue > 1MPa and red<1MPa.

Circumferentially arching force networks (more clearly developed around the shaft in the crushable case) shield the pile shaft surface (at r/R=1) from the higher radial stresses developed at greater r/R. This circumferential arching leads to more weekly developed radial force networks close to the shaft.

It is shown that the DEM is a numerical tool that can offer new insights into the stress conditions developed around piles penetrating in sand. The good match between the DEM and both experimental and FEM results support the reliability of the proposed micromechanical modelling approach.

References

THE UNIVERSITY of EDINBURGH
School of Engineering
Policy and Innovation Group

ORE Supergen
Offshore Renewable Energy

Investigating the value to the UK economy of ocean energy: Scenarios to 2050

Introduction

To develop a clear motivation and benchmark against which research can be measured, the Hub will establish three technical scenarios - 'Aspirational ORE Systems' (AOS) which will act as beacons for intended growth in Offshore Wind, Wave and Tidal technology. Each of the defined AOSs will be explored to enable the evaluation of technology innovation needs; potential effect on the UK economy; benefit to fragile regions; ecological impacts of the scenarios. These AOSs are:

A large scale floating future: A multi-GW floating ORE farm, pushing devices into deeper water than those currently targeted, and creating a significant improvement in farm scale via innovative new engineering systems

A scaled-up and safe exploitation of tidal stream: A leap forward in scale for tidal stream systems, progressing the industry from prototype TRL to systems designed for operation in commercial arrays with high confidence in prediction of performance and ecological acceptability

A farm-scale wave energy sector in which the scaling benefits from single to multiple devices are realised, creating the breakthrough in the viability of this technology that is required to achieve commercialisation.

UK Electricity Generation Supply Energy Mix

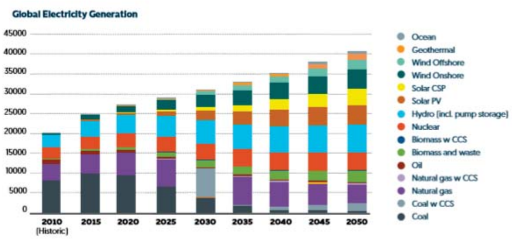

The Integrated MARKAL-EFOM System (TIMES), 2018

Energy Technology Innovation Process

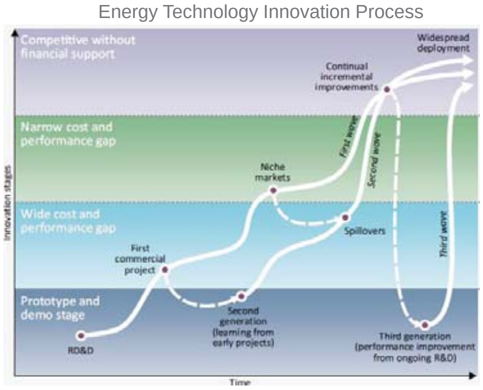

IEA, 2018

Intended Results

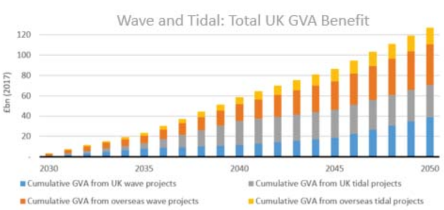

Policy and Innovation Group, 2019

Sector contribution to CO_2 reduction
(baseline vs 2ºC scenario)

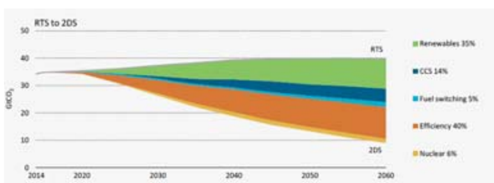

IEA, 2018

Deployment Scenarios

- Definition of characteristics of deployment scenarios using energy systems models ESME and TIMES
- Development of additional energy system models to increase sophistication in the ORE mix estimates
- Determination of optimum energy mixes that, accounting for different levels of system storage, balance offshore wind, wave and tidal technology deployments to produce maximum energy while minimising cost and negative consequences of fluctuating inputs to the grid
- Optimisation of deployment capacity and location of each technology

Technology Innovation

- Identification of technology innovation required to achieve the scenarios
- Activity to inform technology pathways and complement corresponding design and modelling research, more widely in the UK, and beyond.
- Investigation of the practicalities of expanding the range of deployment locations to achieve higher capacity targets
- Examination and presentation of the implications of moving from shallow and intermediate depth operation to deep-water sites, through investigating how technology needs to change and innovate
- Activities here will feed back into deployment scenarios model

Economic Benefit

- Evaluation of the economic prize offered by each scenario, quantified in terms of GVA to the UK economy and number of job-years created, among other metrics
- Identification of the potential benefit to be gained through offshore wind O&M activity and whole supply chain for wave and tidal.
- Investigation of how ORE activity will engage with, reinvigorate, and ultimately benefit marginalised coastal communities

Ecological Assessment

- Ecological impact assessment, Life-Cycle Cost Assessment (LCA) of Global Warming Potential (GWP), Energy Return on Investment (EROI) and Energy Payback Time (EPBT) of devices and deployed arrays of each scenario
- Employment of the Ecological Trade Offs tool-kit to assess the range of economic options examined the previous task within a natural capital approach
- Identification and use of approaches for evaluating how devices, array design, and O&M activities affect the environment

References
ETI, ESME, 2018;
IEA, Energy Technology Perspectives 2017, 2018;
Policy and Innovation Group, Wave and Tidal Energy: The Potential Economic Value, 2019

EPSRC
Engineering and Physical Sciences Research Council

UNIVERSITY OF ABERDEEN

UNIVERSITY OF PLYMOUTH

University of Strathclyde

MANCHESTER 1824
The University of Manchester

C Cochrane
Charlotte.cochrane@ed.ac.uk
H Jeffrey
Henry.jeffrey@ed.ac.uk

Machine learning for power system impedance estimation

Kamyab Givaki
Edinburgh Napier University
k.givaki@napier.ac.uk

INTRODUCTION

- The high amount of converter interfaced sources (e.g Wind) impacts the stability of the system, especially in a weak grid with high inductive impedance.
- The knowledge of the grid impedance at the connection point of the converter to the grid (PCC) is essential for improving the control strategy and overall grid stability by either changing the control action or re-tuning the controller.
- In micro-grids, a variation of impedance is an indication for islanding or grid connection mode operations.
- Furthermore, the knowledge of grid impedance will be useful to improve the power quality, detection of the fault location, ground faults and grim unbalanced operation.
- Methods to estimate impedance of power network can be classified into passive and active methods or combination of these two.
- The passive methods are known to be 'non-invasive' and active methods are 'invasive'.
- The active methods are invasive as a disturbance signal is injected to the grid. Then the signal processing techniques are used to estimate the impedance of the grid.
- Passive methods do not need any disturbance injection, and the available information of the non-characteristic current and voltage at the PCC is used to estimate the grid impedance. Hence, performance of the power system is not degraded using passive methods.
- The use of data-driven models have been successfully demonstrated in applications demanding for real-time estimation of the targets values.
- Both the passive and active impedance estimation methods have shortcomings for power system applications. The passive methods can become inaccurate, and the active methods impact power quality.

Methodology

- The first step of estimation process is to select a set of features for representing the system.
- A Random Forest (RF) model is chosen due to its capability in the prediction of multiple output values simultaneously.
- RF requires several numbers of hyper-parameters to be set.
- These parameters are tuned for the simulated data to achieve the highest possible accuracy.
- The model optimisation is performed using an evolutionary multi-objective NSGA-II algorithm to tune the RF model for accurate estimation of both R and X.
- In each genome (a selection of hyper-parameters), the configured model is trained and tested using 10-fold cross-validation.

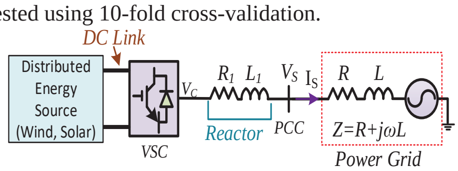

Fig. 1. Schematic block diagram of the test system

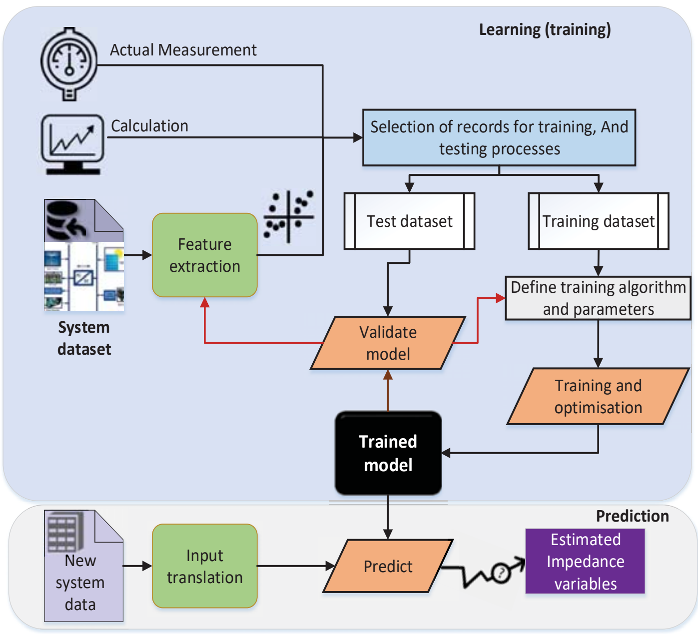

Fig. 2. General schematic diagram of supervised learning

Results

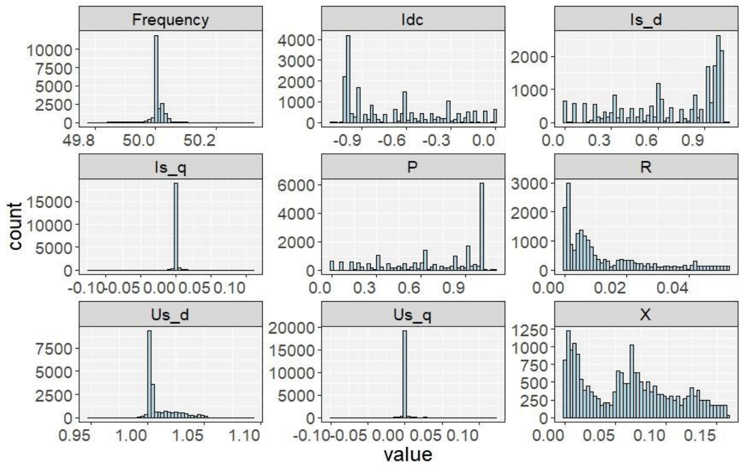

Fig. 3. Distribution of features for the simulated system

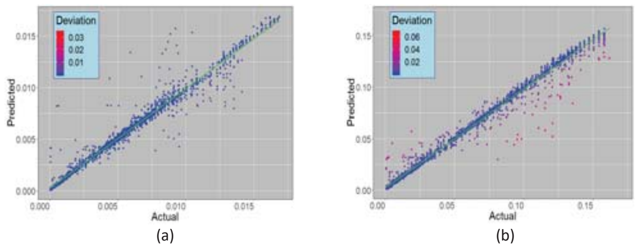

Fig. 4. Predicted vs actual values for a) resistance and b) inductive reactance.

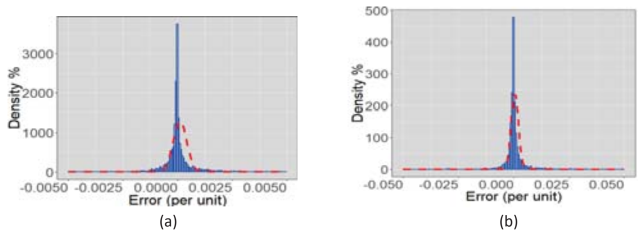

Fig. 5. Histogram of error for a) resistance and b) inductive reactance.

- Root mean square error (RMSE) and R2 are 0.0015 and 0.99 for resistance and 0.0054 and 0.98 for inductive reactance.
- The mean time spent for prediction of one record is calculated as 0.3ms which makes it an ideal model to be used for real-time impedance estimation

CONCLUSIONS

- The random forest model used for estimation of the two components of the impedance, namely, resistance and inductive reactance.
- Current and voltage in the stationary reference frame (dq- axis), active power, DC link current and the frequency at PCC are used as the inputs for the random forest model.
- The model optimisation is performed using an evolutionary multi-objective NSGA-II algorithm to tune the RF model for accurate estimation of both R and X.
- The proposed method does not require any external signal injection; thus, the power quality is not compromised. Furthermore, the model results show that the estimation accuracy is very high.

Numerical Models of a Floating Hinged Raft Wave Energy Converter

Siya Jin, Deborah Greaves, Martyn Hann

University of Plymouth

This research aims at building proper numerical models for a floating hinged raft wave energy converter (WEC) to estimate its dynamic responses. Two methods are used: (1) a fully non-linear CFD model based on ANSYS/LS-DYNA; (2) a linear/ partial non-linear time-domain model based on WEC-Sim. The CFD model is firstly validated by comparing with the experimental data for a fixed raft. The numerical results fit well with the experimental data. A floating hinged WEC is then built in the CFD tank. The performance of the WEC is well predicted by CFD method and the pitch resonance is well captured. The results are also compared with the linear results derived by engineers from MaRINET2. As expected, the WEC response is over-predicted by linear method. This concludes the importance in future work to carefully take consideration of the non-linear terms in models by WEC-Sim.

CFD VALIDATION BY FIXED RAFT

- A fixed raft designed by Mocean Energy ltd is used to validate the capability of CFD model.

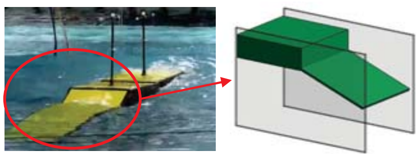

- Wave elevation, on-hull loads and water splashing are compared between CFD and experiment data.

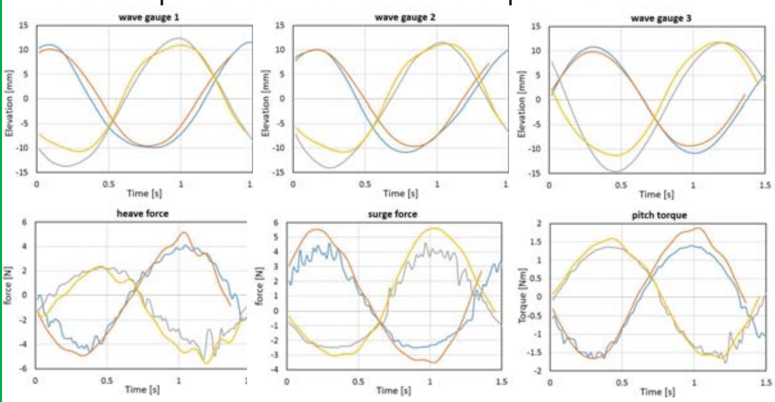

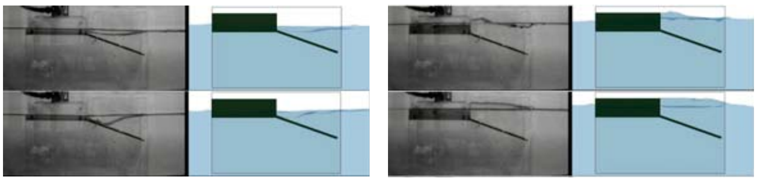

CFD MODEL-FLOATING HINGED WEC

- A full scale floating hinged WEC is built in the numerical wave tank. The mesh solution is designated with large density in the structure-fluid interaction zone and coarse elements near the boundaries. Below shows the half model. The hinge point is on the bow of the yellow raft.

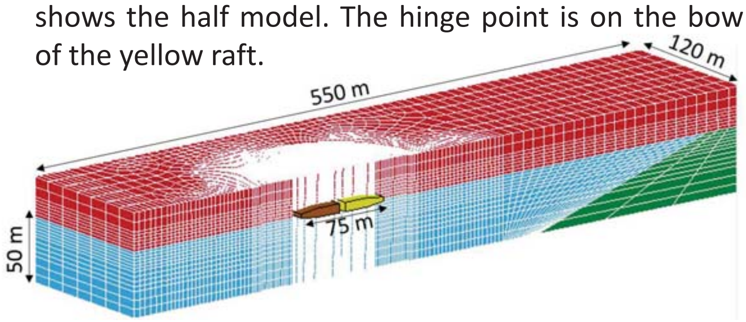

- Regular wave series are tested with wave height H = 1.8 m and wave period T = 6 to 10 s. The aim is to investigate the dynamic responses against varying waves and to capture the resonance.

- The pitch resonance is captured at T = 7 s where the hinged WEC rides almost on a full wave length. Below shows the dynamic response under resonance.

- The hinged WEC synchronously follows the wave motions leading to smaller relative pitch responses under long waves. Below is an example at T = 10 s.

- The pitch RAO at hinge is extracted based on CFD and is compared with the linear results from MaRINET2 using InWave.

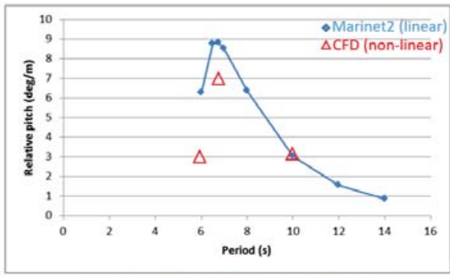

Figure 14: relative pitch RAO of the undamped raft model N°9

CONCLUSION AND FUTURE WORK

Validated by physical tests, the CFD approach shows its feasibility in simulating the structure responses induced by waves. Compared with the CFD results, the dynamic responses of the hinged WEC can be over-predicted by the linear model, especially under resonance. Hence, the non-linear terms should be carefully considered while developing the time domain models based on WEC-Sim. The figures show the models built in WEC-Sim.

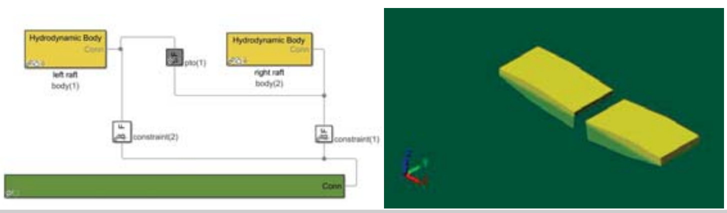

ACKNOWLEDGEMENT

Thanks are expressed to the technicians by MaRINET2 project for designing the hinged WEC and sharing the data with us.

Near wake characteristics comparison of a tidal stream turbine with URANS-AL model

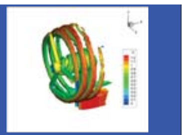

Wei Kang (PDRA)
wei.kang@Manchester.ac.uk
School of Engineering, University of Manchester, UK

ABSTRACT

Wake development has a great impact on performance of downstream turbines and ecological change when tidal turbines are installed in arrays. In this paper, velocity deficit profile and turbulent characteristics are studied using URANS-AL model in comparison with experimental data in near-wake region. The results show that the URANS-AL model agrees well with experiment in wake velocity profile. However, there is great disparity for turbulent kinetic energy comparison in which tip vortex correction for turbulence should be considered in AL model.

Motivation

-Assess actuator line model for wake prediction
-Turbulence characteristics near wake region
-Turbulence changes causing disruption to marine populations

Unsteady flow changes local to array

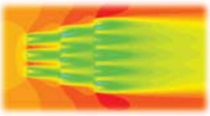

-- to predict --

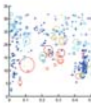

Changes from individuals - up to marine populations

Results and analysis

1. Wake velocity profile comparison

-The wake profile from CFD agrees well with the experiment for the tip shear and wake recovery velocity near the tip
-Disparity near wake tip shear becomes significant as flow is propagating downstream due to the dissipation

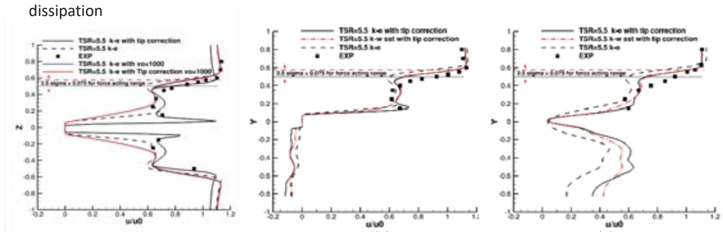

X=0.1D transverse direction | X=0.5D vertical direction | X=1D vertical direction

Fig 1 Wake velocity profile comparison between CFD and EXP

2. Near-wake turbulence characteristics analysis

Experimental velocity data is used to analyze near wake turbulence characteristics. Herein the turbulence is characterized by ambient turbulence, development from ambient turbulence and turbulence induced by coherent structure(e.g., periodic vortex from tip).

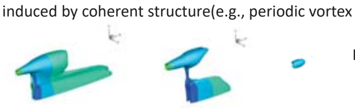

Fig 2 TKE isosurface with k=0.01(left), k=0.05(mid) and k=0.1(right)

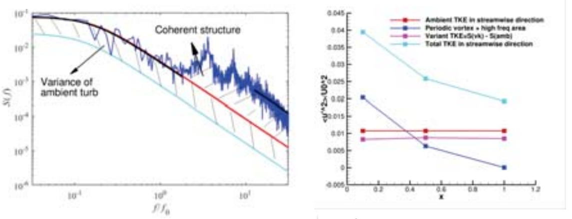

Fig 3 Near-wake turbulence characteristics from experimental data

3. Near-wake turbulence kinetic energy comparison between CFD and experiment

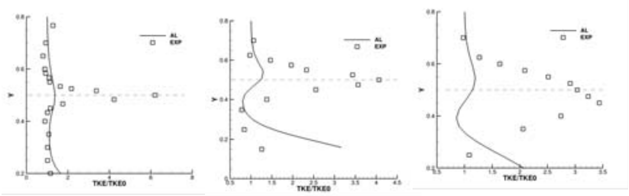

X=0.1D, vertical profile | X=0.5D, vertical profile | X=1D, vertical profile

Fig 4 Near-wake turbulence kinetic energy comparison

Exp TKE: $\frac{1}{2}\langle u'^2\rangle + 2\cdot\frac{1}{2}\langle v'^2\rangle$ where u' and v' is the measured velocity in streamwise and transverse direction

AL TKE: modelled k in k-epsilon RANS model

Numerical Methods

The STREAM Code

- Finite-volume, incompressible solver
- Pressure-velocity coupling: SIMPLE
- Surface-fitting moving mesh (free surface / sediment bed)
- Advanced RANS turbulence models
- Parallelisation: blockwise domain decomposition + MPI

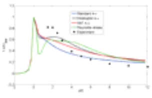

[1]

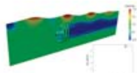

Actuator Line Model

Requirements:
- lift and drag coefficients $C_L(\alpha,r)$, $C_D(\alpha,r)$
- chord distribution $c(r)$
- blade twist distribution $\beta(r)$

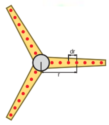

Momentum sink: $\mathbf{F}_p = \frac{1}{2}\rho U_{rel}^2 (c\Delta r)(C_L \mathbf{e}_L + C_D \mathbf{e}_D)$

-BODY FORCES distribution $\mathbf{f}(\mathbf{x}) = \mathbf{F}_p \frac{e^{-(\mathbf{x}-\mathbf{x}_p)^2/\sigma^2}}{\sigma^3\pi^{3/2}}$

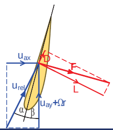

Model description

IFREMER's flow channel[2]

– Mean flow velocity is about 0.8m/s
– Flow channel scale: 10D(streamwise)x1.66D(vertical)x3.33D(transverse)
– Blockage ratio: 0.2

X-MED Turbine parameter

– Rotor diameter D=1200mm
– Tower height: 0.83D
– Tower diameter: 0.085D
– Tower axis to rotor plane: 0.4D
– Nacelle total length: 0.853D

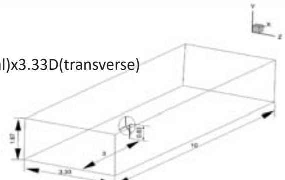

Turbine model being tested at the IFREMER flume with the LDV [2]

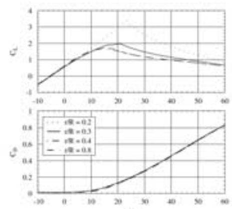

Airfoil database (from Bahaj, radius distribution is not the same)

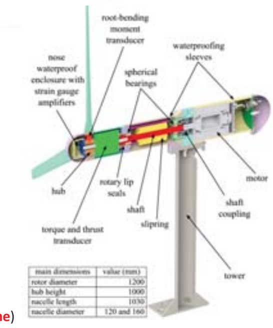

Conclusions

– AL-URANS model for a single tidal turbine is evaluated for wake prediction with the experimental data.
– The velocity profile near wake agrees well with the experimental results. However, the wake deficit with CFD method shows slightly wider downstream.
– The turbulence can be characterized by ambient turbulence, development from ambient turbulence and turbulence induced by coherent structure(e.g., periodic vortex from tip).
– There exists great disparity in near wake region for turbulent kinetic energy comparison. It indicates that URANS-AL model can only capture the ambient turbulence development but fail to describe the tip vortex structure in turbulent mixing.

On-going work will focus on the tip vortex correction for turbulence prediction in AL model.

Acknowledgements & references

Acknowledgements:
The authors would like to acknowledge the support of the EPSRC Supergen Offshore Renewable Energy Hub.

References:

[1] Apsley, D. D., T. Stallard and P. K. Stansby (2018). "Actuator-line CFD modelling of tidal-stream turbines in arrays." Journal of Ocean Engineering and Marine Energy 4(4): 259-271.

[2]. Payne, G. S., T. Stallard and R. Martinez (2017). "Design and manufacture of a bed supported tidal turbine model for blade and shaft load measurement in turbulent flow and waves." Renewable Energy 107: 312-326.

[3]. Payne, G. S., T. Stallard, R. Martinez and T. Bruce (2018). "Variation of loads on a three-bladed horizontal axis tidal turbine with frequency and blade position." *Journal of Fluids and Structures* 83: 156-170.

Plate anchors for offshore floating facilities – Soil – anchor – floating system interactions

Dr Katherine Kwa & Prof David White

UNIVERSITY OF Southampton

Background

A variety of anchoring and mooring systems hold offshore floating renewable energy structures in place

These embedded foundation systems withstand large numbers of variable cyclic loads due to the wave and wind forces acting on the renewable energy structure

Research has shown that the soil around these foundations can strengthen from the sustained and cyclic loading and this can add capacity to the foundations

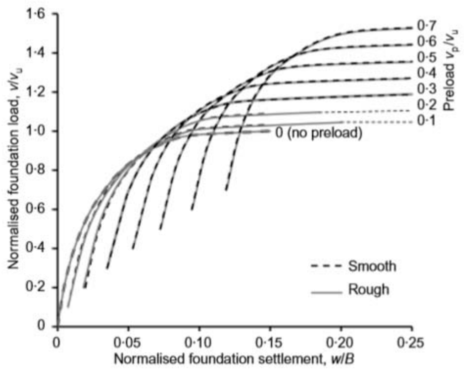

Normalised load vs settlement response to failure following preloading and consolidation. (Gourvenec et al., 2014)

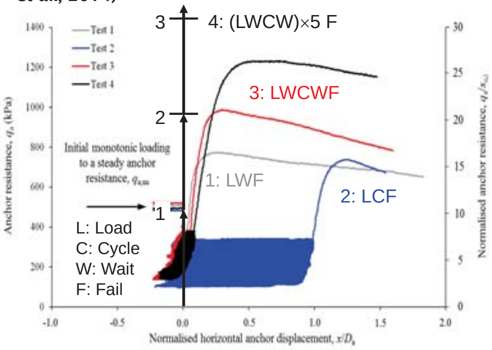

Gains in anchor resistance due to increases in soil strength during cyclic loading (Zhou et al. 2019)

If these gains in capacity are harnessed, then more efficient and cost effective anchoring and mooring can be designed and used

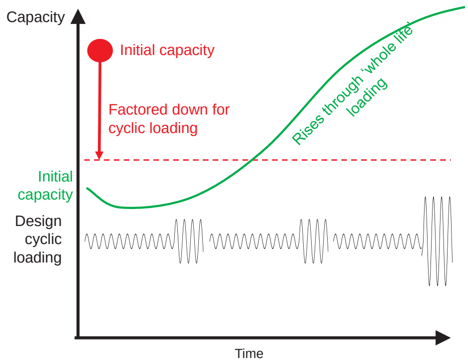

Potential rise in capacity of anchor system

Aims

To improve the foundation design for anchoring and mooring systems of offshore floating renewable energy structures.

Gain a better understanding of the soil behaviour around embedded plate anchors when they are cyclically loaded

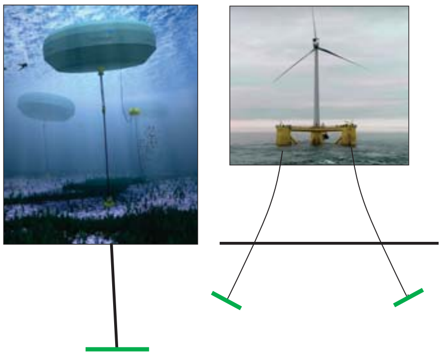

Embedded plate anchors holding wave energy devices and floating wind turbines in place

Add the interaction of the soil and plate anchor mooring system into existing models currently used to capture the behaviour of floating systems, to better model the behaviour of floating offshore renewable energy structures

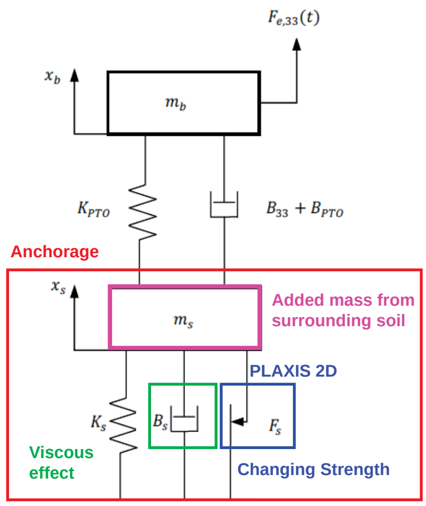

Addition of soil behaviour (in red) to the anchoring system of a simple WEC model (Aquilina, 2019)

Current Work

Using finite element analysis, in PLAXIS 2D, to investigate the soil behaviour around embedded plate anchors

Benchmarking

Checked PLAXIS 2D solutions with analytical solutions for ultimate bearing capacity of surface footings: Nc = 2+π and embedded footings: Nc = 3π + 2

Typical embedded footing failure mechanism obtained in Plaxis 2D

Results

Proceeded to investigate the behaviour of the soil above and below the plate during a set of preload, wait, fail (LWF) cases

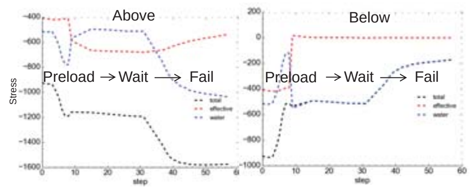

Stresses above and below the plate during the LWF case in PLAXIS 2D

Observed relative increases in soil strength above the plate and decrease in soil strength below the plate

The net effect is the difference between the gain in strength above and loss of strength below the plate

The relative gains in soil strength above the plate increased with larger preloads

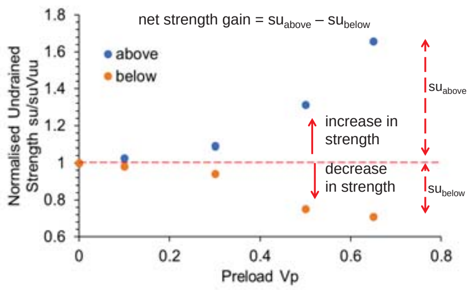

Changes in soil strength above and below the embedded plate anchor

Future Work

Centrifuge modelling experiments

Integration of the interaction between soil and plate anchor mooring system using soil-like elements in WEC-Sim

References

Aquilina, J. P. (2019). MSc Thesis, Mooring- seabed coupling of wave energy converters, Univ. Southampton.

Gourvenec, S. M., Vulpe, C., & Murthy, T. G. (2014). A method for predicting the consolidated undrained bearing capacity of shallow foundations. Géotechnique, 64(3), 215-225.

Zhou Z., O'Loughlin C.D. White D.J. & S.A. Stanier 2019. Changes in plate anchor capacity under maintained and cyclic loading due to consolidation effects. Géotechnique, Ahead of Print.

Supergen Offshore Renewable Energy

EPSRC Engineering and Physical Sciences Research Council

Email: k.a.kwa@soton.ac.uk

Supergen ORE Hub Early Career Researcher Forum
5-7th November 2019

Real-time wave energy control based on machine learning

Liang Li

Department of Naval Architecture, Ocean & Marine Engineering, University of Strathclyde

Abstract

A predictive real-time latching control strategy is developed and implemented to a heaving point-absorber to increase its power extraction. An artificial neural network, which is trained with the machine learning algorithm, is used to predict future wave force. The smart control increases the power extraction by locking and realizing the WEC according to the control command. The control efficiency and its sensitivity to the prediction error are investigated.

Introduction

Compared with other offshore renewable energy resources, wave energy has the advantage of high power density and all-day availability. Owing to these advantages, wave energy is regarded as a prospective solution to the sustainable generation of clean energy.

In order to maximise the power extraction of WECs, the wave energy control is commonly used to regulate the WECs. Henriques et al. [1] applied real-time latching control to an oscillating-water-column WEC. Son and Yeoung [2] used the model predictive control to enhance the absorption efficiency. Nevertheless, these control schemes are not applicable in the natural world, since they assumed that the wave forces in the near future were already known. Therefore, a predictive real-time controller must be developed for application in real practice

Model description

This work considers a heaving point-absorber. A state-space model is developed to simulate dynamics of the point-absorber.

$$\dot{\boldsymbol{x}} = \boldsymbol{\gamma} \cdot \boldsymbol{x} + \boldsymbol{\eta}$$

$$\boldsymbol{\gamma} = \begin{bmatrix} 0 & 1 & \mathbf{0} \\ -\dfrac{K}{M+m} & -\dfrac{D+\beta c}{M+m} & -\dfrac{\boldsymbol{C}}{M+m} \\ \mathbf{0} & \boldsymbol{B} & \boldsymbol{A} \end{bmatrix}, \boldsymbol{\eta} = \begin{bmatrix} 0 \\ \dfrac{F_{wave}}{M+m} \\ \mathbf{0} \end{bmatrix}$$

The energy absorption is given by

$$P = \frac{1}{T}\int_0^T D \cdot \dot{z}(t,\beta)^2 dt$$

Predictive real-time control

The Hamiltonian H is introduced to maximise the power extraction

$$H = D\dot{z}^2 + \boldsymbol{\lambda} \cdot (\boldsymbol{\gamma} \cdot \boldsymbol{x} + \boldsymbol{\eta})$$

According to the Pontryagin maximum principle, the optimal control command β is the one maximising the Hamiltonian at every time step. The Hamiltonian reaches the maximum value on condition that

$$\beta = \begin{cases} 1 & \lambda_2 c\dot{z} < 0 \\ 0 & otherwise \end{cases}$$

The state vector $\boldsymbol{\lambda}$ follows the following relationship

$$\dot{\lambda}_i = -\frac{\partial H}{\partial \boldsymbol{x}_i}(t, \boldsymbol{x}, \beta), i = 1,2,..,n$$

$$\boldsymbol{\lambda}(T) = \mathbf{0}$$

A feedforward neural network is developed for the wave force prediction. The network is trained with the machine learning to predict wave force through the real-time measurement of wave elevations. Please refer to [3] for more details

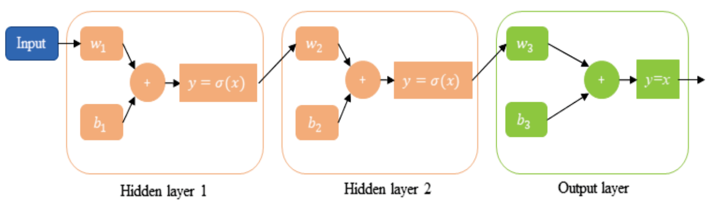

Fig 1. Artificial neural network

Fig.2 summaries the work flow. The first step is to teach the neural network how to predict future wave force based on the wave elevations. The trained neural network is thus able to forecast future wave force, which will be inputted to the control to give the control command. The WEC then operates under the regulation of the controller.

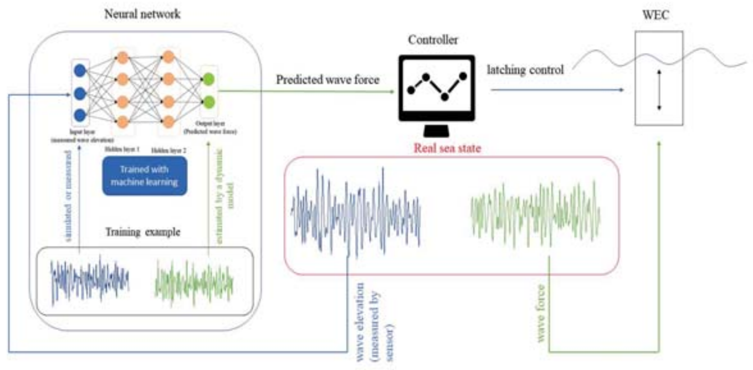

Fig 2. flow chart

Simulation results

Table 1 shows the power extraction of the WEC. It is good to see the power extraction is increased substantially with the predictive control algorithm.

Table 1. Power extraction in random waves

	Hs=2m,Tp=6s	Hs=2.5m,Tp=8s	Hs=3m,Tp=10s
Without control	10 kW	15 kW	18 kW
With control	12 kW	30 kW	50 kW

Since the prediction is not perfect, the prediction error will have an influence on the control efficiency. It is shown the wave force amplitude error is nearly negligible, whereas the wave force phase error dominates the control efficiency.

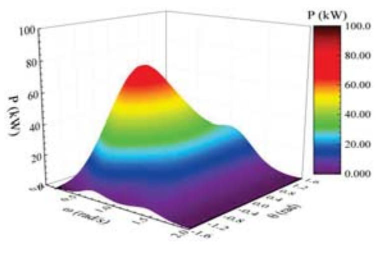

Fig 3. Phase error effect

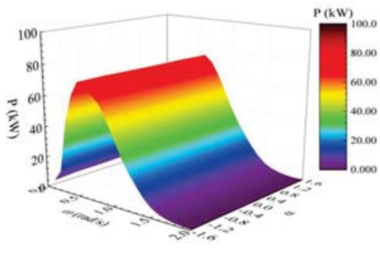

Fig 4. Amplitude error effect

Conclusions

A predictive real-time latching control with consideration of wave force prediction is developed. It is manifested that the controller can enhance the power extraction of a heaving point-absorber significantly, even without the knowledge of wave forces in the future. Therefore, the developed real-time controller is applicable to a realistic industrial WEC product.

References

[1] J.C.C. Henriques, L.M.C. Gato, A.F.O. Falcao, E. Robles, F.X. Fay, “Latching control of a floating oscillating-water-column wave energy converter”, Renewable Energy 90 (2016) 229-241.

[2] D. Son, R.W. Yeung, Optimizing ocean-wave energy extraction of a dual coaxial-cylinder WEC using nonlinear model predictive control, Applied Energy 187 (2017) 746-757.

[3] L. Li, Z. Gao, Z.M. Yuan. On the sensitivity and uncertainty of wave energy conversion with an artificial neural-network-based controller. Ocean Engineering 183 (2019) 282-29.

Future offshore floating wind platform – challenge and opportunity

Yibo Liang
University of Strathclyde

Background

To date, all the demonstrated concepts for offshore floating wind development are still based on a simple “one turbine one platform” system, where each turbine will be mounted on a single floating platform. However, this system will cause lots of waste on manufacturing the floating platform, and increase the cost of transportations as well as onsite installations. Therefore, a question has been raised: “Could two or more turbines seat on one platform?” By doing so, the usage of one platform could serve for multi turbines which significantly decreases the cost of transportation and installation for a wind farm. Additionally, this could have a better performance on space utilization.

For future offshore wind developments, very large floating structure (VLFS) can be potentially considered as a promising alternative for their potential to maximize the power generating capacity and to drastically reduce some dangerous and costly offshore operations.

Figure 1. Artist’s impression of the hybrid 50MW platform. (Energy Island Ltd. 50MW Platform. 2009)

Challenges

When head waves passing a barge type VLFS, a strong hydrodynamic bending moment could be observed.

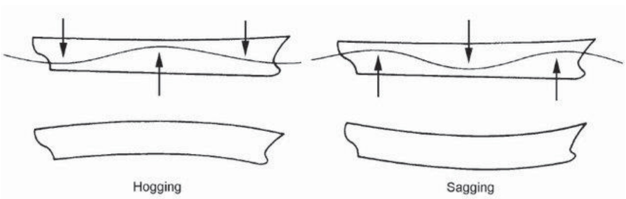

Figure 2. Strong bending moment could be observesed at hogging and sagging

Solution to reduce the maximum bending moment - Hinge

Bending moment

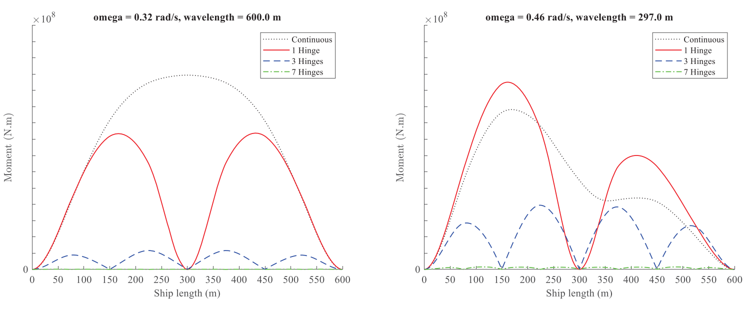

Figure 3(a) Trade off between bending moment and displacement.

For a VLFS, one of the possible solution to reduce the maximum bending moment on the structure is to introduce interconnected hinges onto the structure. Thus, a single-module VLFS is changed to a hinged multi-module VLFS. At the hinge joint, no internal bending moment is generated. This could potentially reduce the maximum bending moment acting on the whole VLFS.

Motion displacement

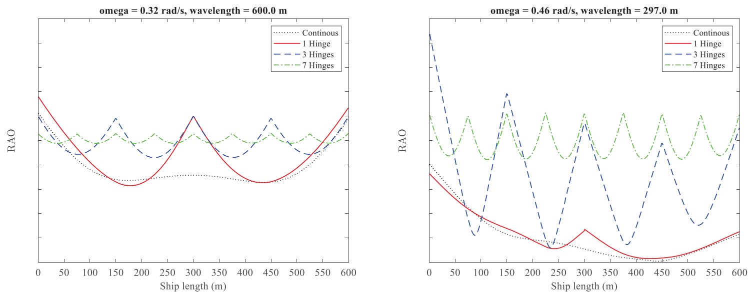

Figure 3(b) Trade off between bending moment and displacement.

Applying wind turbines on the VLFS

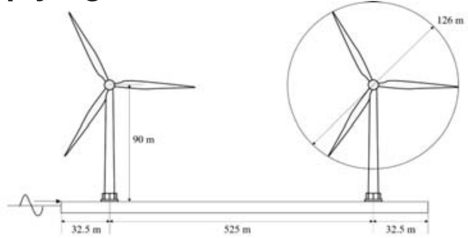

Figure 4. Sketch of two 5 MW wind turbines built on the VLFS.

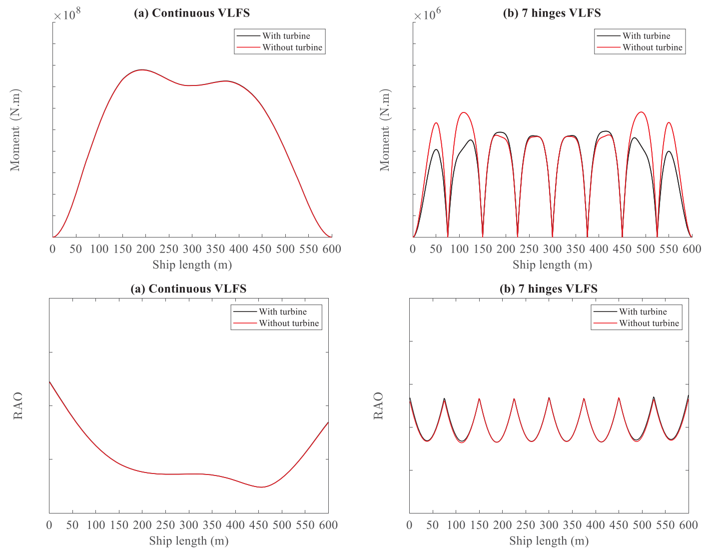

Figure 5. Comparison between with turbines and without.

Preliminary observations

A multi hinged VLFS design will be benefited by adding the wind turbines onto the structure, especially in reducing the bending moment. By reducing the bending moment, more the selections of material for building the VLFS can be applied. Unlike the traditional steel VLFS built for the airport (continuous VLFS), the offshore wind VLFS with multi-hinges has more flexibilities on the structure design and the selections of material.

Development of novel low-cost methods to understand environmental processes in highly energetic ORE sites

Lilian Lieber[1], Alex Nimmo-Smith[2], Melissa Costagliola-Ray[3], Emma Whettall[4], Nicholas Horne[1], and *others in the Bryden Centre*

[1] Queen's University Belfast, Marine Laboratory, Portaferry, Northern Ireland, UK, Contact: **l.lieber@qub.ac.uk** & **nhorne01@qub.ac.uk**
[2] University of Plymouth, Marine Institute, Plymouth, England, UK Contact: **alex.nimmo.smith@plymouth.ac.uk**
[3] University of the Highlands and Islands, ERI, Thurso, Scotland, UK, Contact **melissa.costagliola-ray@uhi.ac.uk**
[4] University of the Highlands and Islands, SAMS, Oban, Scotland, UK, Contact: **emma.whettall@sams.ac.uk**

THE BRYDEN CENTRE
ADVANCED MARINE AND BIO-ENERGY RESEARCH

The Bryden Centre project is supported by the European Union's INTERREG VA Programme, managed by the Special EU Programmes Body (SEUPB)

Interreg
Northern Ireland - Ireland - Scotland
European Regional Development Fund
EUROPEAN UNION

UNIVERSITY OF PLYMOUTH
QUEEN'S UNIVERSITY BELFAST
University of the Highlands and Islands
Oilthigh na Gàidhealtachd agus nan Eilean
Supergen Offshore Renewable Energy

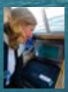

Lilian is a Post-doctoral Researcher combining hydroacoustic tools (echosounders, ADCPs, sonar) with visual survey techniques to understand marine predator occupancy patterns.

@LilianLieber @AlexNimmoSmith @CostaglioRay @Ewhettall @NicholasSHorne @BrydenCentre_EU

high-resolution Flow patterns

How can we characterise and extract fine-scale coherent structures in eddy-dominated flows?

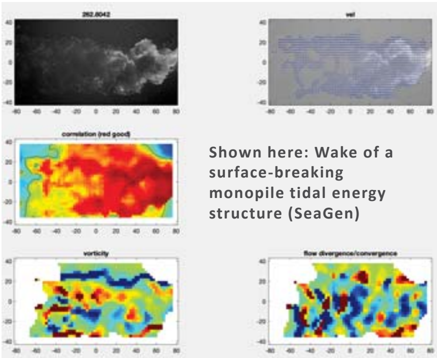

Shown here: Wake of a surface-breaking monopile tidal energy structure (SeaGen)

Mapping surface velocity fields from drone hovers using PIV (particle image velocimetry) techniques to capture highly evolving physical features (vorticity, upwelling/downwelling) to investigate associations between foraging seabirds and highly localised, dynamic flow features at each timestep.

How do surface flow structures measured by GPS drifters & time-series photography compare to concurrent ADCP transects?

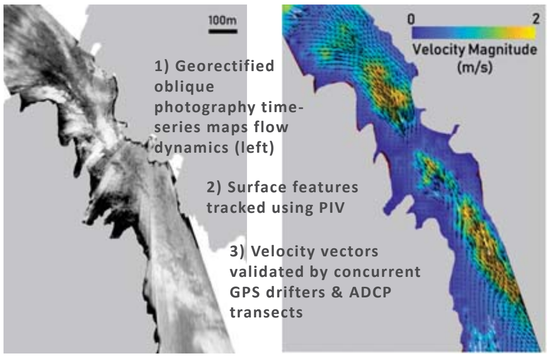

Emma's PhD explores the nature of the tidal resource for community-scale tidal stream energy, with a focus on the spatial variability of small-scale flow structures using a combination of georectified oblique photography, GPS drifters, and PIV techniques.

fine-scale Marine predator site usage

Prey or hydrodynamic features?

What determines marine predator foraging patterns in highly energetic environments?

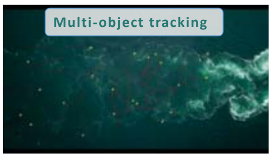

Shallow plunge-diving seabirds forage around turbulent structures & shallow upwellings [1], while seals make use of flow-reversals and avoid highly turbulent areas, such as in the mid-channel during peak flows [2].

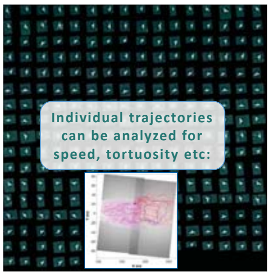

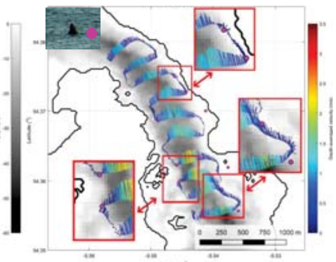

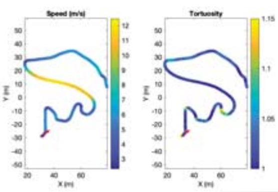

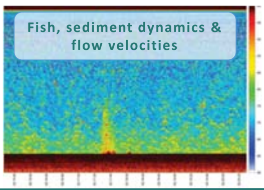

How do seabirds use tidal sites? Vantage point surveys from the shore are compared to concurrent UAV (drone) transects to map foraging distributions:

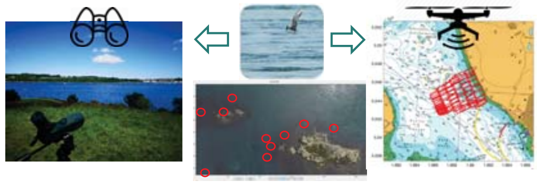

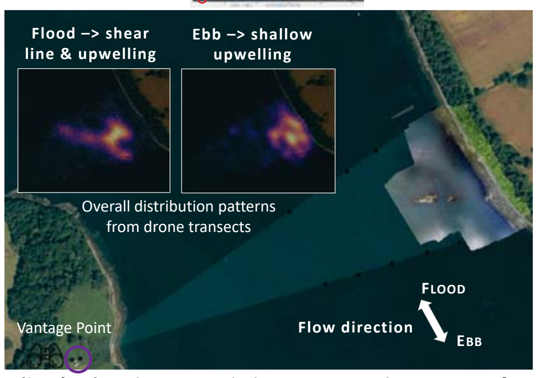

Melissa's PhD aims to optimize vantage point surveys for seabird monitoring around tidal energy sites.

With a rapid expansion in offshore renewable energy (ORE), a broader perspective on their ecological implications is timely to predict environmental change.

In combination, our research highlights the ecological importance of fine-scale hydrodynamic structures & localized physical forcing around man-made structures placed in unsteady flows.

Interested in working with us? The Bryden Centre serves a stewardship role through environmental research activities to help accelerate renewable energy.

[1] **Lieber L,** Nimmo-Smith WAM, Waggitt JJ & Kregting L (2019) Localised anthropogenic wake generates a predictable foraging hotspot for top predators. *Commun. Biol.* **2**, 123

[2] **Lieber L**, Nimmo-Smith WAM, Waggitt JJ, Kregting L (2018) Fine-scale hydrodynamic metrics underlying predator occupancy patterns in tidal stream environments. *Ecological Indicators* **94,** 397-408

http://go.nature.com/2FZ2vyS

Collision Risk

Can a simulated approach help us model underwater collision risk? Which ecologically-important parameters are needed as input?

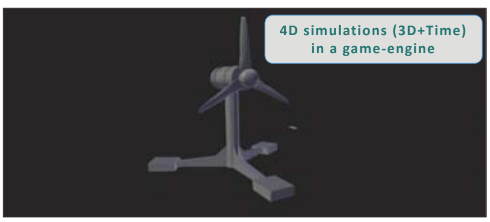

Nick's PhD aims to build models in the game engine Blender to simulate underwater collision risk of marine fauna (e.g. seals) with moving components of tidal energy structures.

HOME-Offshore WP 1.2 - Offshore Wind Turbine Multi-physics Modelling

Zi Lin, Debora Cevasco and Maurizio Collu (work package leader)

Department of Naval Architecture, Ocean & Marine Engineering, University of Strathclyde

Background & Motivation

- **Operation and maintenance (O&M) account for a substantial part in wind turbine cost**
- **Advanced machine learning technologies will assist fault detection & identification, but having difficulties in understanding the cause of these faults**

5 MW & 10 MW HOME-Offshore Wind Turbine

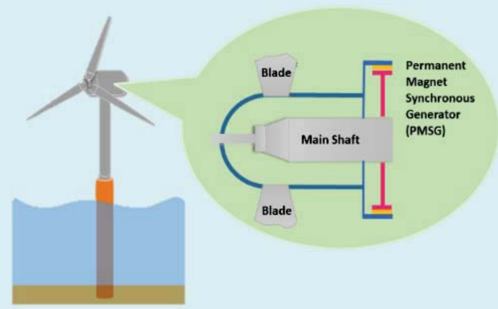

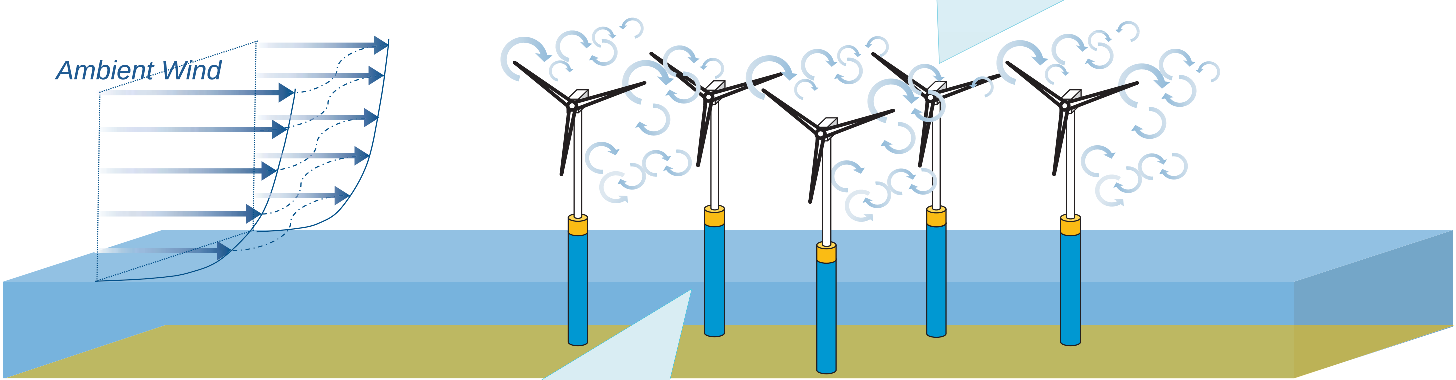

A Single Wind Turbine AHSE-PMSG Coupled Model of Dynamics

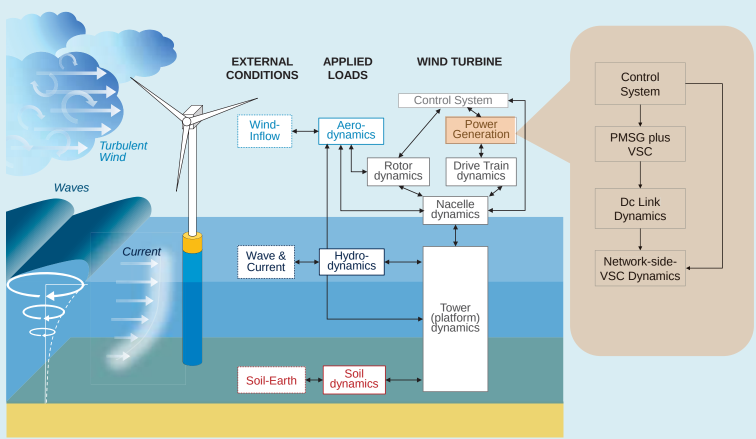

Research Aim

- **To develop a holistic advanced AHSE-PMSG model of dynamics for offshore wind turbines**
- **For better supporting wind turbine condition monitoring and robotic inspection, to understand how the mechanical failure and electrical failure will have an influence on each other**

Results

- **The figure on the right shows a comparison of the statistical values of the power distribution between steady wind (Simplified AHSE-PMSG) and turbulent wind (Advanced AHSE-PMSG).**
- **Generally speaking, using a simplified AHSE-PMSG model with steady winds fails to address the substantial range of instantaneous power outputs experienced by the wind turbine for a given average wind speed**

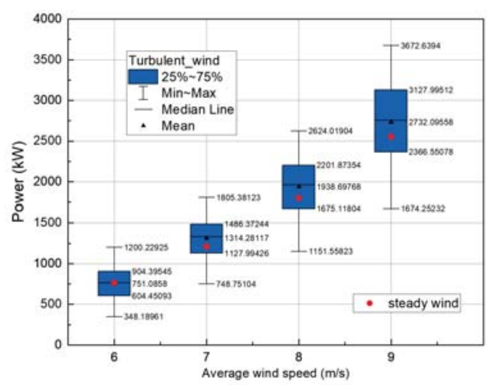

ACKNOWLEDGEMENTS

The work presented is supported by the UK Engineering and Physical Sciences Research Council (EPSRC) HOME-Offshore project (EPSRC Reference: EP/P009743/1). The second author is also supported by grant EP/L016303/1 for Cranfield University, the University of Strathclyde and the University of Oxford, Centre for Doctoral Training in Renewable Energy Marine Structures - REMS (http://www.rems-cdt.ac.uk/) from the UK Engineering and Physical Sciences Research Council (EPSRC).

REFERENCES

Jonkman JM, Jonkman BJ. FAST modularization framework for wind turbine simulation: Full-system linearization. J Phys Conf Ser 2016;753. doi:10.1088/1742-6596/753/8/082010.

Individual Pitch Actuator Monitoring of Offshore Wind Turbines

Dr. Yanhua Liu & Prof. Ron J. Patton

University of Hull, Y.Liu@hull.ac.uk, R.J.Patton@hull.ac.uk

© EPSRC Prosperity Partnership
EP/R004900/1

Background

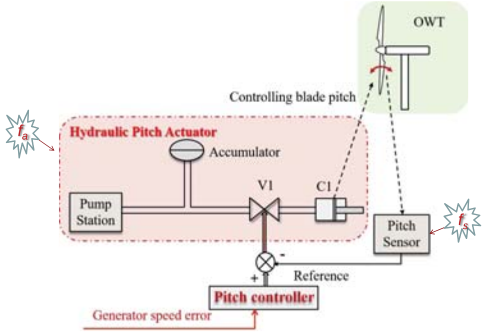

A single hydraulic pitch system with faults

Hydraulic pitch systems (actuators & sensors) are prone to faults, affecting the power output, structural loads etc. The faults lead to approximately 22% of annual turbine downtime.

Individual pitch actuator monitoring includes:

- Actuator "stuck" faults
- Actuator incipient dynamic changing faults, i.e. hydraulic leaks, pump wear, high air content.
- Pitch sensor faults.

★ Research Aim ★

Propose appropriate pitch actuator monitoring strategy to enhance wind turbine reliability & sustainability.

Work Overview

A. Fault monitoring for pitch actuator stuck (PAS) faults

➢ **Fault Description**

After PAS occurs, the pitch actuation output will stay constant no matter what the pitch reference is. Moreover, the pitch measurement will be a fixed value.

➢ **Fault Monitoring Strategy**

A fault detection and isolation (FDI) strategy using Kalman filter is proposed. The pitch system output estimates are generated from Kalman filter and a residual is used to detect the faults.

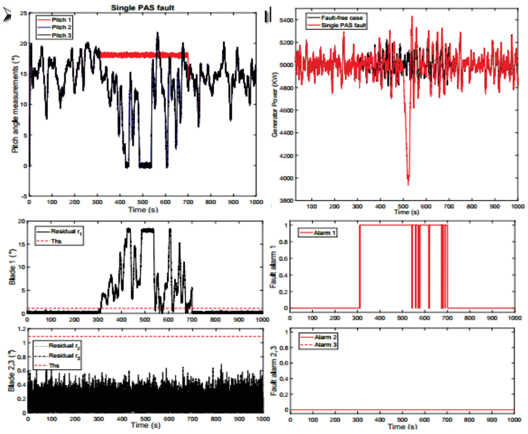

Pitch angle measurements

Generator power output in the faulty case

Fault detection result

B. Fault monitoring for actuator incipient dynamic changing faults

➢ **Fault Description**

Hydraulic leakage due to improper management of oil, pump wear from continuous operation & high air content in oil will cause pitch actuator system has changed dynamics. This leads to <u>slow pitching & unstable outputs</u>.

Step response of one pitch actuator

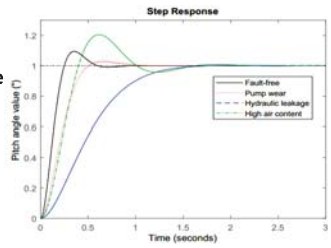

➢ **Fault Monitoring Strategy**

A Sliding Mode Observer strategy is used to obtain pitch fault estimates.

➢ **Results (3 pitch actuators suffer from different incipient faults)**

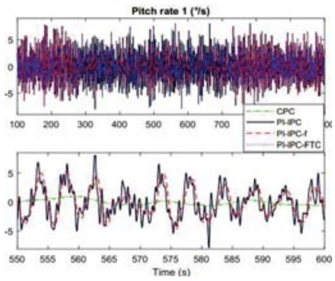

Pitch rate of blade 1

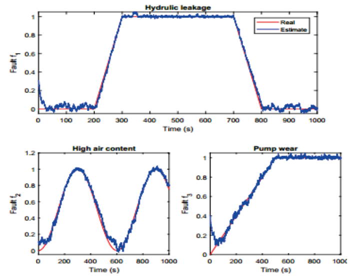

Fault estimation results

C. Fault monitoring for pitch sensor faults

➢ **Fault Description**

Pitch sensor faults lead to incorrect pitch position readings. Hence, the pitch control system cannot guarantee that each blade is in the reference position. <u>4 different sensor faults</u> considered: Biased sensor, stuck sensor output, total and partial sensor faults.

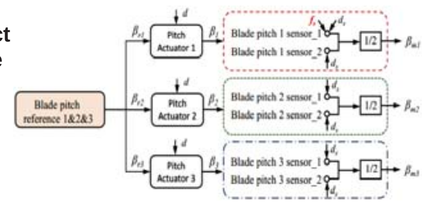

Pitch system with sensor fault f_s

➢ **Fault Monitoring Strategy**

A robust "unknown input observer" using H infinity optimization theory is used for accurate sensor fault estimation.

➢ **Results (single sensor fault on pitch 1 sensor_1 & collective pitch control)**

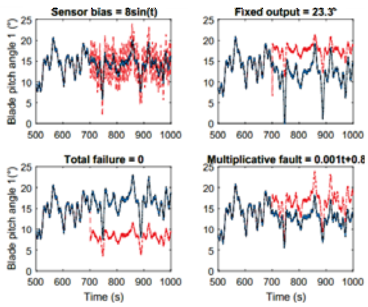

Sensor faults

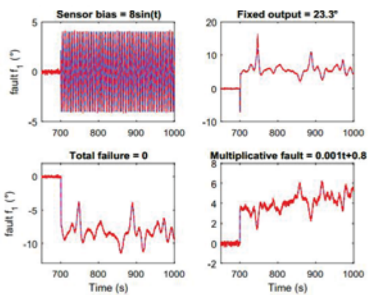

Fault estimation results

Future Work

❖ On-line Monitoring of blade root and tower bending moment sensors considering sensor redundancy and appropriate control.

❖ Verification and validation of fault monitoring designs in the NREL FAST 5MW wind turbine model using Monte Carlo campaign, with and without faults.

EPSRC Engineering and Physical Sciences Research Council
SIEMENS Gamesa RENEWABLE ENERGY
Ørsted
The University Of Sheffield.
Durham University
UNIVERSITY OF HULL

Programmable Flexible Materials for Mooring and Station Keeping

Dr. Saeid Lotfian
Mr. Iman Ramzanpoor (MEng.)
Prof. Margaret Stack
Prof. Feargal Brennan

Background

Renewable marine energy has emerged as a centrepiece of the new energy economy, because of its abundance, regularity and to be environmentally - friendly. Floating offshore platforms could solve the problem of using high depth water to extract energy by using mooring systems. The moorings of wave devices, floating tidal turbines and ultimately floating offshore wind turbines will be subjected to the combined excitations of hydrostatic, hydrodynamic, aero-dynamic and electromechanical forces driven by a combination of wave, tidal, wind and network interactions. The performance and structural responses of the energy converters are influenced by the behaviour of the moorings.

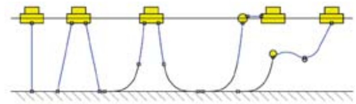

Research Aim and Objectives

- Investigate the potential of programmable flexible materials to provide adaptive behaviour and improved, sympathetic mooring response.
- Study the dynamic mooring systems to create a definition of adaptive strain/stiffness.
- A combination of smart materials and structure solutions would be investigated in tandem with mooring design analysis.
- Define the elements and capabilities required for a larger collaborative initiative to fully explore the potential for programmable flexible materials for mooring and station keeping.

Results

Mooring hardware components are included:

- Chain, Wire or Rope or their combination;
- Anchors or Piles;
- Connectors.

In this study, different mooring line diameters were considered and the maximum RAO (Response Amplitude Operator) motion amplitude achieved when the waves have an incident angle of 0 degrees (head sea).

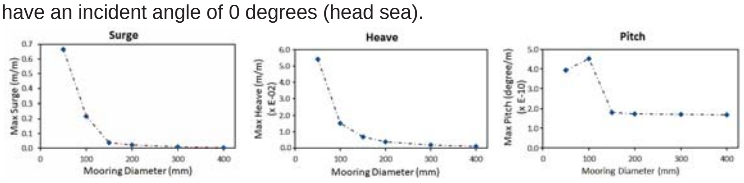

Site-specific spectral densities of the sea elevation process can be determined from available wave data. It could be represented by the JONSWAP spectrum which is an empirical relationship that defines the distribution of energy with frequency within the sea. The following figures demonstrate the JONSWAP spectrum superimposed to the pitch and surge RAOs related to moored TLB floating structure when the mooring lines diameter alter.

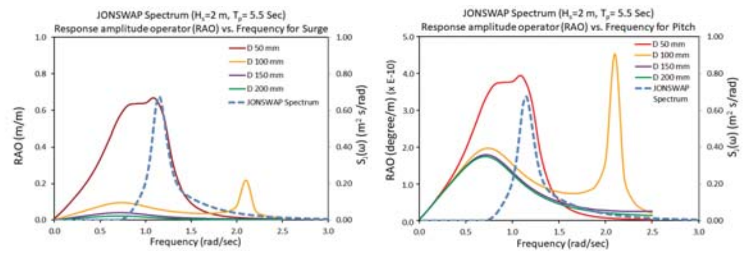

Stiffness of Tension Leg System

- The restoring force and moments exerted by the mooring system are **nonlinear** in translational and rotational displacements of the floating structure.
- The mooring loads exerted on the platform will depend on the mooring system **geometry**, **configuration**, and **cable properties**.
- The stiffness matrix of a mooring system composed of multiple lines is evaluated by summing the stiffness matrices of the individual lines.

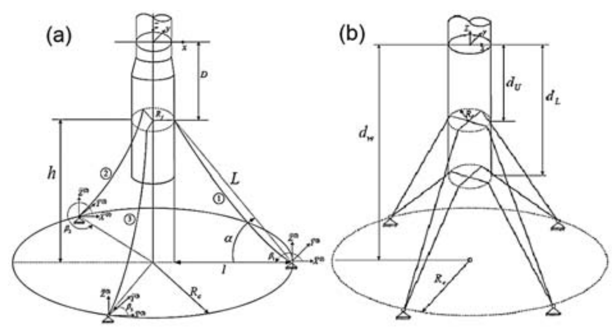

(a) Symmetric *n*-tethered system (sketched for n = 3 for clarity) referred to as 'taut-leg' mooring system for taut lines; (b) Taut Line Buoy (TLB) floating structure concept with four-anchor.

$$K_m = \begin{bmatrix} K_{11} & 0 & 0 & 0 & K_{15} & 0 \\ 0 & K_{22} & 0 & K_{24} & 0 & 0 \\ 0 & 0 & K_{33} & 0 & 0 & 0 \\ 0 & K_{42} & 0 & K_{44} & 0 & 0 \\ K_{51} & 0 & 0 & 0 & K_{55} & 0 \\ 0 & 0 & 0 & 0 & 0 & K_{66} \end{bmatrix}$$

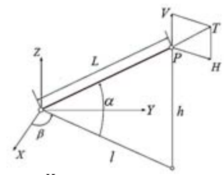

$$K_I = EA/L$$

$$K_{11} = 0.5n\left(\frac{T}{L}(1+\sin^2\alpha) + K_I\cos^2\alpha\right)$$

$$K_{15} = -n\left(\frac{T}{2L}(D + D\sin^2\alpha + R_f\sin\alpha\cos\alpha) + \frac{K_I}{2}(D\cos^2\alpha - R_f\sin\alpha\cos\alpha)\right)$$

$$K_{33} = n\left(\frac{T}{L}\cos^2\alpha + K_I\sin^2\alpha\right)$$

$$K_{44} = n\left[T\left(D\sin\alpha + \frac{1}{2}R_f\cos\alpha\right) + 0.5\frac{T}{L}\left((R_f\cos\alpha + D\sin\alpha)^2 + D^2\right)\right] + 0.5nK_I(D\cos\alpha - R_f\sin\alpha)^2$$

$$K_{66} = n\frac{TR_f}{L}(R_f + L\cos\alpha)$$

$K_{22} = K_{11}$ $\quad K_{24} = -K_{15}$ $\quad K_{42} = K_{24}$ $\quad K_{51} = K_{15}$ $\quad K_{55} = K_{44}$

Materials and Structures

The main method to **manage the stress** in mooring system is to **control the stiffness** in mooring line.

- *Hybrid Materials*

- *Tube-Core*

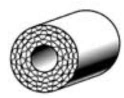

- Possible collaboration:

Further Steps

- **Erosion:**

Design of erosion experiments to evaluate the degradation of the structure;

- **Fatigue:**

The mooring system is subject to highly cyclic, non-linear load conditions;

- **Creep:**

Wire, fibres and ropes show an irreversible deformation (creep) behaviour that is strongly dependent upon load and temperature;

- **Hysteresis and heat build up:**

The energy induced by cyclic loading is dissipated (hysteresis) in the form of heat.

Acknowledgements

We would like to acknowledge the financial support from the Engineering and Physical Sciences Research Council (EPSRC) through Centre for Advanced Materials for Renewable Energy Generation (CAMREG) project.

Relevant References

1. Al-Solihat, M.K. and M. Nahon, *Stiffness of slack and taut moorings*. Ships and Offshore Structures, 2016. **11**(8): p. 890-904.
2. *DNV-OS-J101 offshore standard*, *in Design of offshore wind turbine structures*, 2010.
3. *DNV-RP-H103 modelling and analysis of marine operations*, 2011.
4. Thies, P.R., et al., *Mooring line fatigue damage evaluation for floating marine energy converters: Field measurements and prediction.* Renewable Energy, 2014. **63**: p. 133-144.
5. Ramachandran, G., et al. *Investigation of response amplitude operators for floating offshore wind turbines*. in *The Twenty-third International Offshore and Polar Engineering Conference*. 2013. International Society of Offshore and Polar Engineers.
6. Chakrabarti, S., *Handbook of Offshore Engineering (2-volume set)*. 2005: Elsevier.

Motion damping of floating offshore wind turbines using porous materials

Dr. Ed Mackay, Prof. Lars Johanning

Renewable Energy Group, College of Engineering, Mathematics and Physical Sciences, University of Exeter

E.Mackay@exeter.ac.uk

Introduction

- A key challenge for developing cost-competitive floating offshore wind is design of stable platforms
- Increased platform motions lead to reduced energy yield and increased fatigue loads on the turbine
- Adding a porous outer layer to a floating platform can reduce platform motions without significant increase in size and cost.
- This work describes model tests with a TLP wind turbine with a porous outer layer.

Semi-submersible floating wind turbine. Credit: NREL

TLP model design

- Simplified 1:50 scale TLP model, based on NREL OC4 design, with rotor-nacelle represented as lumped mass
- Comprises solid inner column and porous outer column
- Tested in 7 configurations:
  - Base case: no outer cylinder
  - 6 outer cylinders: 2 diameters x 3 porosities (0%, 15%, 30%)
- Total mass and COG constant in all configurations
  - Outer cylinder weight compensated by variable inner mass
  - Pitch and roll motions negligible so change in moments of inertia not important
- Main objective is to validate numerical predictions and demonstrate proof of concept - model is not intended to be realistic design.
  - Freeboard of central column and outer cylinder increased to improve linearity
  - Base cylinder diameter increased to accommodate changeable outer cylinders

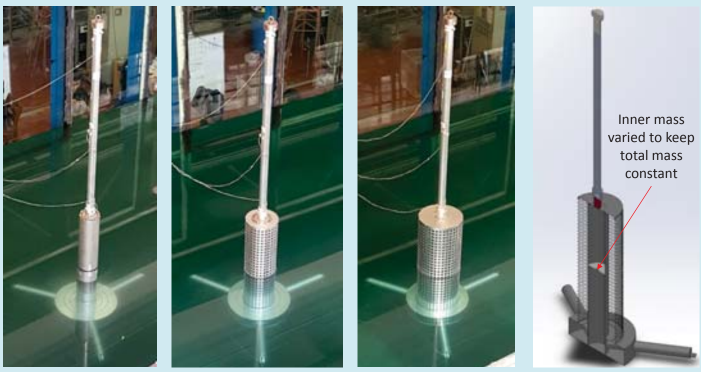

Tank test results

- Two sets of tank tests were conducted at Dalian University of Technology (China) and the FloWave tank at University of Edinburgh
- Measurements were made of
  - 6-DOF platform motions
  - Mooring line tensions
  - Tower bending moments.
- Tests comprised regular and random waves and focused groups
- Adding solid outer cylinder moves resonant response to lower frequency and increases peak response
- Damping from wave radiation and vortex shedding is small at low frequencies
- Increasing porosity of outer cylinder increases damping and reduces peak response

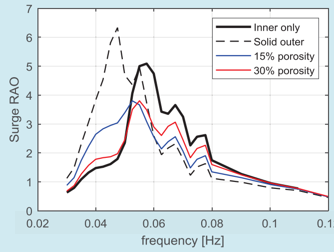

Surge RAOs in regular waves for 4 configurations

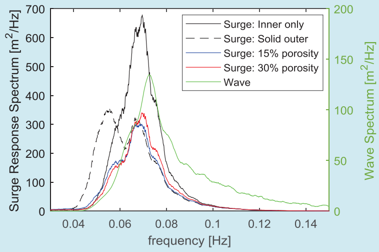

Surge response spectra in a sea state with Hs=8m, Tp=14s

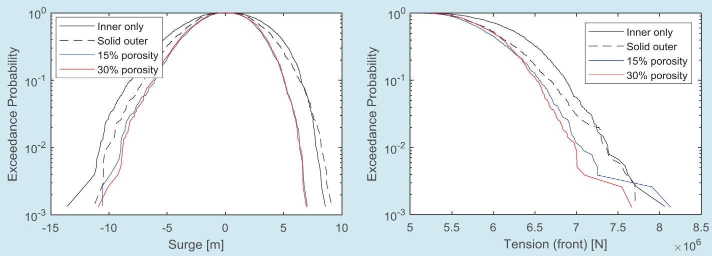

Exceedance statistics in a sea state with Hs=8m, Tp=14s. ***Left:*** *surge motion.* ***Right:*** *Front line mooring tension.*

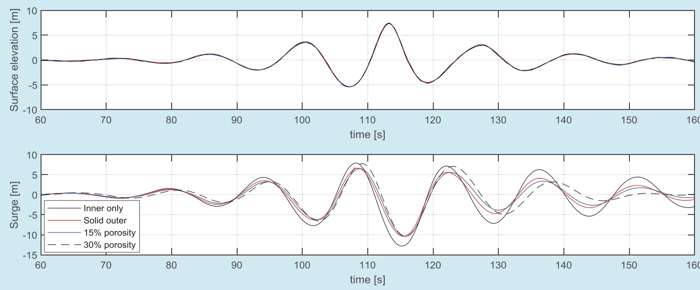

Surge response in a focused group with H=12.8m, Tp=14s

Conclusions and further work

- Results from tank tests indicate that adding a porous outer layer to a floating platform can reduce motion RAOs, leading to reduced loading and potentially increased energy capture
- Tank test results will be compared to numerical predictions from an iterative boundary element method (BEM) model [1, 2]
- The BEM model will be used to investigate more practical designs and quantify impact on motion response and structural loads

References

[1] Mackay EBL, Feichtner A, Smith RE, Thies PR, Johanning L. Verification of a Boundary Element Model for Wave Forces on Structures with Porous Elements. Proc. 3rd Int. Conf. on Renewable Energies Offshore (RENEW 2018), Lisbon, Portugal

[2] Mackay EBL, Johanning L, Qiao D, Ning D. Numerical and experimental modelling of wave loads on thin porous sheets. Proc. 38th Int. Conf. Ocean, Offshore, Arctic Eng. (OMAE2019), Glasgow, Scotland

Acknowledgements:

This work was funded through EPSRC (UK) grant EP/R007519/1 and the National Natural Science Foundation of China grant 51761135011

Flow control for wind turbine airfoils

Dr Marinos Manolesos
Swansea University
marinos.manolesos@swansea.ac.uk

Motivation

Passive flow control is the definite choice for wind turbine manufacturers due to its simplicity, robustness, ease of application and effectiveness.

Vortex Generators

Vortex Generators are flow separation control devices that generate streamwise vortices, which energize the flow locally. Their small size, at the order of the local boundary layer height, renders the study of the resulting flow challenging both experimentally and numerically.

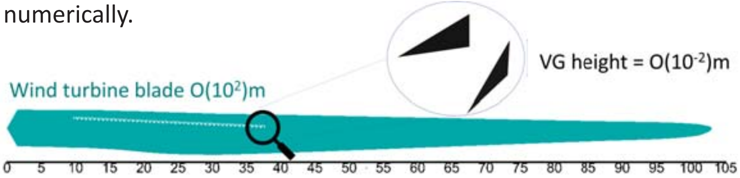

The most **detailed experimental database** on Vortex Generator flows has been created through **extensive Wind Tunnel testing**. It has proved Vortex Generator efficiency and has been widely used for **CFD benchmarking**.

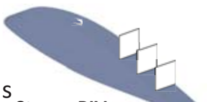

Vortex Generator efficiency

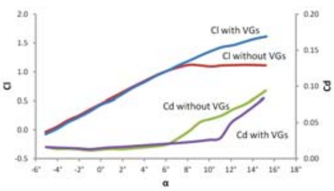

Airfoil with VGs: Aerodynamic performance

Experimental database for CFD validation

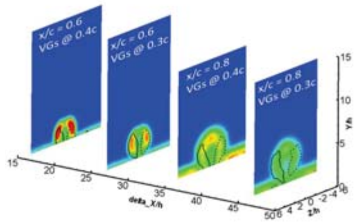

$\overline{w'w'}$ *– Normal Re Stress in the wake of the VGs*

Flatback Airfoil Flow Control

As **flatback airfoils** are included in wind turbine blade design **drag reduction devices** are becoming increasingly popular for wind turbines. An **innovative drag reduction device** has been proposed, that outperforms existing devices by 20%. **Further development** is planned within **2020**.

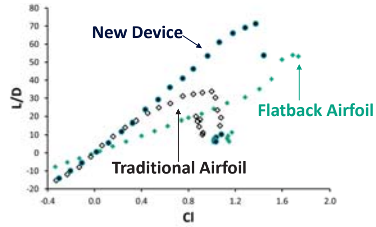

Active camber morphing wings

Morphing trailing edge devices can generate large, smooth and continuous changes in camber distribution. **Simultaneous PIV and DIC measurements** reveal the **fluid – structure interaction** for such flows

Conclusions

Results are indicative of the **Wind Turbine expertise** available at Swansea University and the possibilities of our new Wind Tunnel.

References

J. of W. Eng. & Ind. Aerod., Vol 142, 130-148

AIAA Journal, Vol. 54, No. 11, 3382-3396.

J. Aircr. 52 (2015) 307–319. doi:10.2514/1.C032725.

Swansea University Wind Tunnel

- Commissioned in 2016
- Re number 3.1M per m
- Maximum speed 50m/s
- 1.5m x 1.0m
- Measurements
  - ✓ Pressure
  - ✓ Velocity
  - ✓ Fluid Structure Interaction
  - ✓ Force – Torque – Vibrations
  - ✓ Flow Visualization
  - ✓ Pitching model motion

Wake structure of tidal stream turbine arrays under increasing flow depth

Pablo Ouro

OuroP@cardiff.ac.uk

Hydro-environmental Research Centre, School of Engineering, Cardiff University, UK.

Motivation

At every tidal site the local environmental conditions related to water depth or bathymetry are different. These can notably change the flow dynamics, e.g. velocity profile distribution or turbulence production, impacting on the energy generation capabilities of tidal stream turbine arrays. Hence, there is a need to individually investigate the layout that maximises the energy generation of the array at any site.

Relatively low submergences, i.e. turbines occupy a great proportion of the water column, can have an immediate effect in the tidal turbine wake dynamics, restricting the wake expansion and thus diminishing wake velocity recovery rate. Consequently, energy generation capabilities from secondary rows can be greatly reduced. Due to this obvious implication, it is necessary to identify and quantify the changes in wake recovery mechanisms depending on the relative water depth, so we can modify the location of the turbines within the array to maximise energy generation.

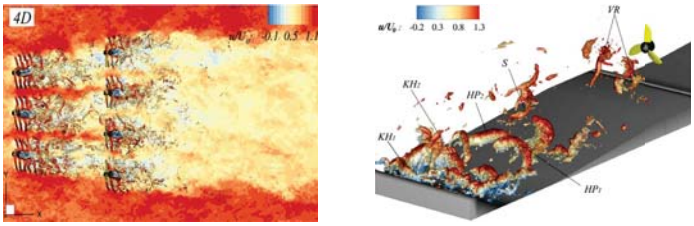

Figure 1. Left: Array of seven tidal turbines simulated using DOFAS [4]. Right: impact of irregular bathymetry on a tidal turbine [1].

Digital Offshore Farms Simulator

DOFAS (Digital Offshore FArms Simulator) is a state-of-the-art in-house code that adopts the method of Large-Eddy Simulation (LES) [1,2,4] to resolve the large-scale flow structures, highly present in tidal turbines hydrodynamics, while the small scales are modelled with the WALE sub-grid scale model.

DOFAS adopts the fractional-step method with a Runge-Kutta predictor is to approximate convection and diffusion terms, and the fluid domain is discretised with a Cartesian mesh using fourth-order central differences to compute velocity fluxes. DOFAS is fully parallelised with MPI and features an immersed boundary method to represent solid bodies, an actuator line model to simulate turbine rotors, a synthetic eddy method to generate artificial turbulence, and local mesh refinement method to refine the grid in the regions of interest.

The validation of DOFAS to predict the hydrodynamics and structural loads in the prototype tidal farms from Stallard et al. [3] can be found in Ouro et al. [4].

Why does water depth play a role in the wake recovery dynamics?

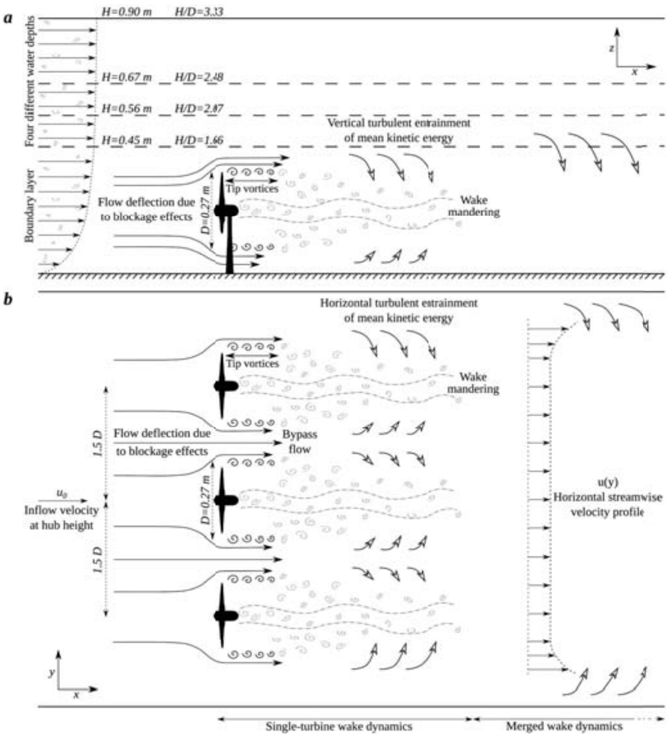

Tidal stream turbine array layouts have to be designed to produce energy under various operating conditions. The operation of tidal turbines differs from wind turbines because of the proximity of vertical bounding layers, i.e. bottom bed and free-surface. Identifying the physical mechanisms involved in the wake and energy recovery, and their evolution under different environmental conditions, in particular at different water depths, is key to design efficient arrays.

Similarly to what has been done in wind farms [5], the terms of the transport equation for mean kinetic energy (MKE) can be analysed (Eq.1). Of special interest is to understand the mechanisms involved in the MKE recovery of MKE focus in which different transport terms are involved. Figure 2 depicts the flow dynamics involved in the recovery of tidal turbine wakes, outlining the turbulent transport of MKE both horizontally and vertically. The latter has proven to be responsible for the energy generation in large wind farms [5] but it is unsure its relevance in tidal farms.

$$\underbrace{\langle u_j\rangle \frac{\partial \langle u_j\rangle^2/2}{\partial x_j}}_{\text{Convective transport of MKE}} = \underbrace{-\langle u_j\rangle \frac{1}{\rho}\frac{\partial\langle p\rangle}{\partial x_i}}_{\text{Transport due to pressure}} + \underbrace{\frac{\partial}{\partial x_j}\left[\upsilon \frac{\partial \langle u_j\rangle^2/2}{\partial x_j}\right]}_{\text{Transport due to viscous stresses}} - \underbrace{\upsilon\frac{\partial^2\langle u_j\rangle^2/2}{\partial x_j^2}}_{\text{Viscous dissipation}}$$

$$- \underbrace{\frac{\partial}{\partial x_j}\langle u_j\rangle\langle u_i'u_j'\rangle}_{\text{Transport due to shear stresses}} + \underbrace{\langle u_i'u_j'\rangle\frac{\partial\langle u_j\rangle}{\partial x_j}}_{\text{Turbulent dissipation (production of tke)}} + \underbrace{\frac{1}{\rho}\langle u_i\rangle f_i}_{\text{Power extracted by turbines}}$$

Figure 2. Schematics of (a) the wake recovery behind a tidal turbine for different submergences and key phenomena involved in the vertical transport of mean kinetic energy. and (b) the wake recovery behind a row of tidal turbines and key phenomena involved in the horizontal transport of mean kinetic energy.

Turbulent transport of mean kinetic energy

Figure 3 presents the profiles of turbulence-induced MKE fluxes averaged over *10D* behind the turbine. In Fig. 3a, positive values indicate downwards flux, and vice-versa, while in Fig.3b, positive values mean MKE transfer towards negative *y*-direction, and vice-versa. Therefore, the fluxes of MKE are oriented towards the centre of the wake behind the turbine, leading to an enhanced wake recovery. Larger the water depths increase the amount of MKE available above the turbine and changes turbulent distribution leading to greater vertical transport of MKE (Fig. 3a) whilst weaker horizontal transport of MKE (Fig. 3b).

These results evidence that under relatively shallow conditions, the vertical expansion of the wake is constrained by the proximity to free-surface changing the turbulence distribution. The spread of turbulent momentum exchange across the water depth is limited by the free-surface, as observed from vertical Reynolds shear stresses *u'w'*. The intensity of these stresses decreases at a faster rate for the shallower conditions. Conversely, levels of horizontal Reynolds shear stresses *u'v'* are greater for shallower flows.

This research shows that arrays performance vary for different environmental conditions, suggesting turbine rows can be clustered more closely for ratios of water depth to turbine diameter approximately over 2.

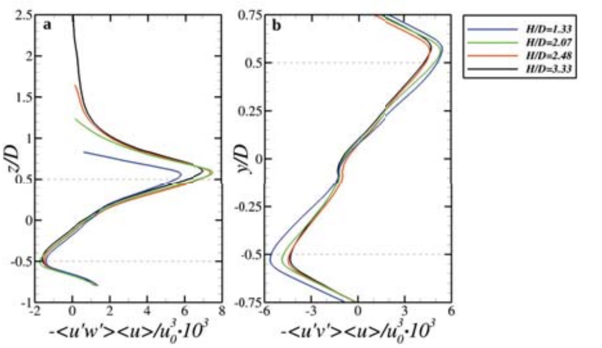

Figure 3. Vertical (a) and horizontal (b) fluxes of mean kinetic energy averaged over the streamwise direction behind the middle turbine in a three in-line array.

References

[1] **P. Ouro**, T. Stoesser. 2019. Impact of Environmental Turbulence on the Performance and Loadings of a Tidal Stream Turbine. *Flow, Turbulence and Combustion*. 102: 613-639.

[2] **P. Ouro**, M. Harrold, T. Stoesser, P. Bromley. 2017. Hydrodynamic performance and structural assessment of a horizontal axis tidal turbine prototype. *Journal of Fluids and Structures. 71: 78-95.*

[3] T. Stallard, R Collins, R Feng, J Whelan. 2013. Interactions between tidal turbine wakes: experimental study of a group of three-bladed rotors. *Phil Trans R Soc A*. 371: 20120159.

[4] **P. Ouro**, L. Ramirez, M. Harrold. 2019. Analysis of array spacing on tidal stream turbine farm performance using Large-Eddy Simulation. *J Fluids Struct*. 91: 102732.

[5] Cal B, Lebron J, Castillo L, Kang H, Meneveau C. 2010. Experimental study of the horizontally averaged flow structure in a model wind-turbine array boundary layer. *J Renew Sust Energy*. 2: 013106.

DATACUBE SERVICES FOR THE OFFSHORE RENEWABLE ENERGY INDUSTRY IN THE UK

Dr. Alberto S. Rabaneda and Dr. Rodney Forster

University of Hull, Faculty of Science and Engineering

SATELLITE APPLICATIONS WITHIN THE OFFSHORE RENEWABLE ENERGY

The collection of samples for analysis and *in situ* measurements at specific locations have been the most common conventional methods for environment and resource monitoring. They can provide accurate information with high temporal frequency, but just for particular points in terms of space. Earth Observation (EO) satellites have the potential to help overcome these limitations, by greatly increasing the spatial coverage of samples. Satellites are a most cost-effective device for ocean observation, providing water quality and sea parameters related information over extensive spatial and temporal scales. The introduction of remote sensing into environmental monitoring provides a novel capability to evaluate, analyse and forecast changes of specific ocean products.

Monitoring of the coastal zone is necessary in order to quantify human activities. Offshore wind farms, tidal and wave power stations need marine and atmospheric environmental information to select optimal sites and to forecast power production. The large-scale construction of offshore renewable energy sites may also have environmental impacts which are still unknown in the long term. These impacts might not be only produced by constructed power devices, but also by the following increase in marine traffic around the area. Hence, an Environmental Impact Assessment (EIA) is compulsory to quantify human impacts.

Thus, EO can be applied with ORE projects for:

1. **EIA projects**
   a. Prediction & Mitigation before construction
   b. Managing & Monitoring during operation
2. **Resource monitoring campaigns**
   a. Before construction
   b. During operation

EO environmental parameters

- Reflectance
- Turbidity
- Suspended Sediment Concentration
- Chlorophyll concentration
- Alga bloom detection
- Eutrophic depth
- Salinity
- Man-made object detection

EO resource parameters

- Sea surface temperature (SST)
- Significant Wave height
- Wave period
- Sea level
- Sea wind vectors at multiple heights
- Surface roughness length
- Currents

DATACUBE STRUCTURE

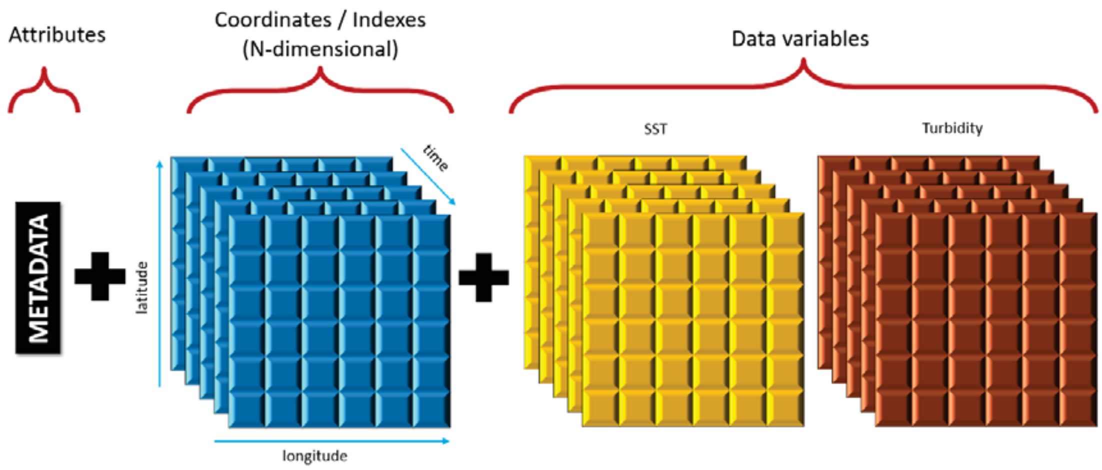

Making the best use of the vast quantities of earth-observing data arising from the Sentinels and other satellites requires new methodologies to merge all the different environmental parameters. A solution in development by different teams for different locations is the Datacube. This new technique will allow time-series analysis and at the same time help find correlations between parameters which will lead to a better understanding of physical processes and the human impact on the environment. The database structure is based in the NetCDF format.

DATA PROCESSING

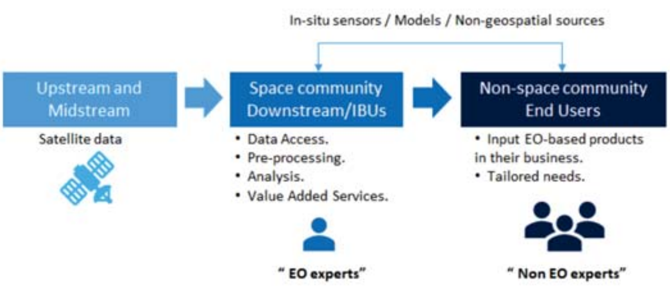

Satellite data is available through the different datahubs from ESA, NASA and other space agencies. This data needs to be processed in order to retrieve physical and environmental parameters. The data processing as well as datacube creation is undertaken by EO experts. Then, the data is made available accompanied by a software for visualization and exportation named EOdatabee.

API GRAPHICAL USER INTERFACE

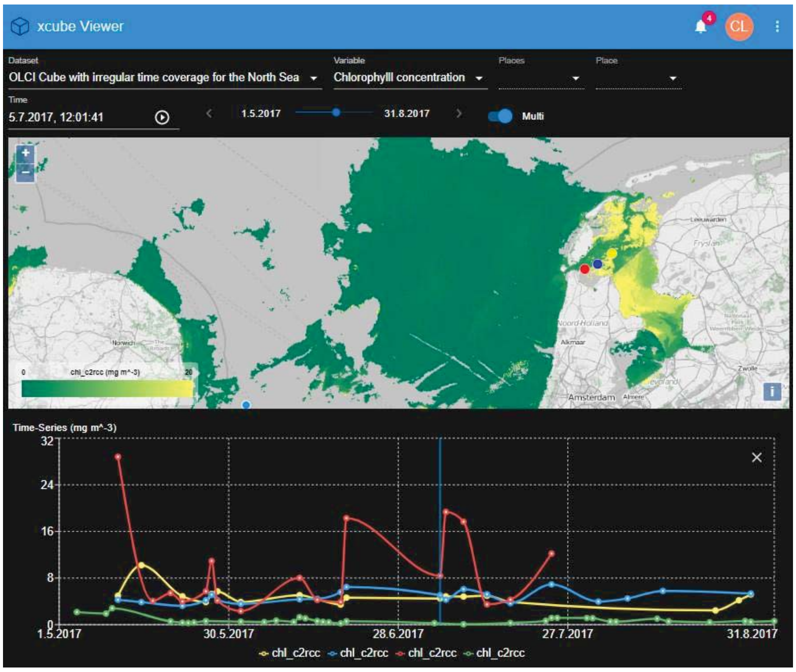

This is an early example of the visualization software, Eodatabee, still under development. The datacube here is named "OLCI Cube with irregular time coverage for the North Sea". The chlorophyll concentration variable was selected and plotted on a map. Four different points for comparison were selected. A time-analysis comparison can also be made with Eodatabee.

The Collaborative Computational Project in Wave Structure Interaction (CCP-WSI)

E. Ransley*[1], D. Greaves[1], L. Qian[2], J. Zang[3], Q. Ma[4], S. Yan[4], G. Tabor[5], C. Jones[6], G. Poulter[6]

*edward.ransley@plymouth.ac.uk, [1]Plymouth University, [2]Manchester Metropolitan University, [3]University of Bath, [4]City University London, [5]University of Exeter, [6]Science and Technology Facilities Council

Introduction

The UK has an outstanding record of research in Wave Structure Interaction (WSI) and good reason to maintain this status, particularly in the light of its leading position in the development of modern offshore renewable energy (ORE) technologies. However, the challenges facing the WSI community in developing the necessary complex, multi-physics, multi-component suit of Computational Fluid Dynamics (CFD) software are significant and represent a goal that can only be achieved through a collaborative code development environment.

In response, a Collaborative Computing Project (CCP) has been established to serve the UK research community in the area of WSI. The project, which began in October 2015, brings together computational scientists, CFD specialists and experimentalists with the shared objective of developing a Numerical Wave Tank (NWT) facility that complements existing and future UK experimental laboratory facilities and supports leading-edge research in marine, coastal and offshore engineering.

Aims and objectives

The CCP-WSI aims to:

- Develop a robust and efficient computational WSI modelling tool
- Build the community of researchers and developers around WSI
- Provide a focus for software development and code rationalisation

Strategy setting

The combined CCP-WSI and SIG-WSI network is a growing international group of over 115 researchers, spanning academia and industry in 5 continents. The group has identified a number of key WSI challenges/priorities and has co-created a roadmap for WSI code development through industry focus group workshops with 75 attendees.

Contributions to knowledge

The CCP-WSI has advanced understanding of the applicability and reliability of WSI through a set of internationally recognised Blind Test series' involving 50 participants. The CCP-WSI Blind Test activities have been presented in dedicated sessions at 3 international conferences with 25 papers published in 3 special issue journals (Figure 3). Over 80 journal publications have been generated by the CCP-WSI team and over 20 presentations have been given at national and international conferences. A number of pilot projects with industry, outreach activities with school children and public audiences have also been delivered.

Figure 1: Images from the 'Introduction to CCP-WSI Code Developments' training event (in collaboration with Queen's University Belfast), Belfast, N. Ireland, 16th September 2019. Clockwise from top left - Attendees enjoying the 'hands-on' training; screenshot from the first tutorial - solitaryWaveMaker; screenshot from the third code development – sixDoFRigidBodyMotion bodyForces; attendees enjoying a tour of the Queen's University facilities.

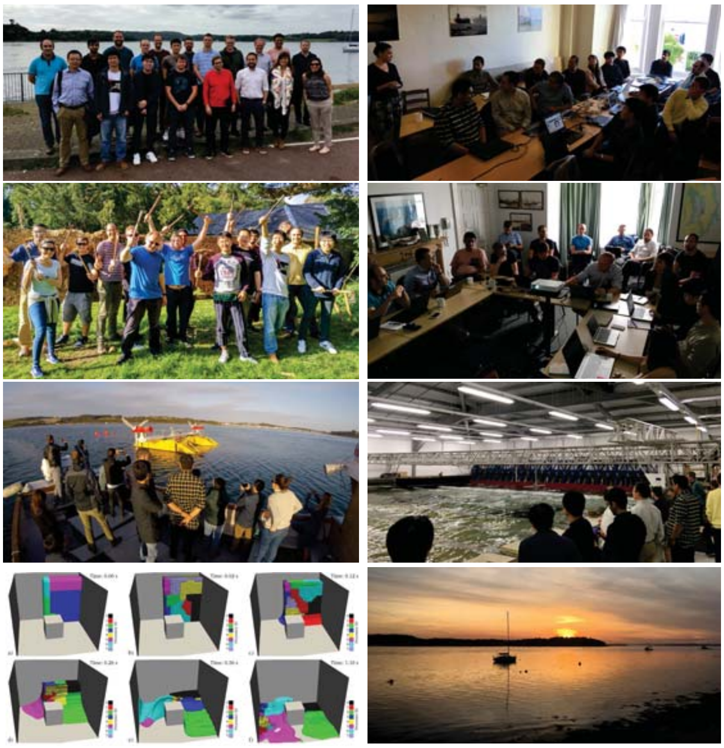

Figure 2: Images from the 1st CCP-WSI Hackathon (in collaboration with Queen's University Belfast), Portaferry, N. Ireland, 16-20th September 2019. Clockwise from top left – Participants of the 1st CCP-WSI Hackathon; participants getting to know each other; advanced training delivered; tour of Queen's University Marine Laboratory; sunset over Strangford Lough; one code development worked on at the event – dynamic load-balancing; boat tour of Strangford Lough; attendees enjoying a spot of axe-throwing and archery towards the end of a productive week.

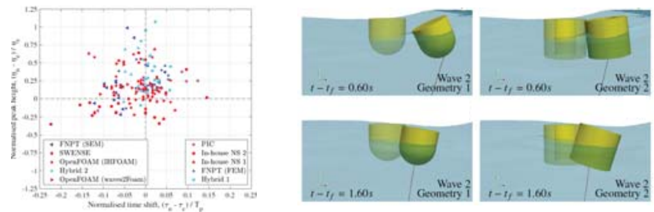

Figure 3: Some results from the CCP-WSI Blind Test Series 1 – focused wave impact with a fixed FPSO (Ransley et al. 2019) (left); snapshots from a contribution to the CCP-WSI Blind Test Series 3 – focused wave interactions with floating structures (Brown et al. 2020) (right).

Strategic software development and support

Training has been provided to the community with 76 attendees, including training in software engineering, specific code development, the use of the CCP-WSI Code Repository and specific WSI developments (Figure 1) and a week-long Hackathon for intense collaborative code development (Figure 2). The CCP-WSI Code Repository and clearing house provides a platform for co-creation and sharing of open-source WSI code for community use, and is maintained by the CCP-WSI Organisation on Github with over 45 users and more than 300 commits. The CCP-WSI Data Repository supports a growing database of benchmarking test cases for community use and validation practices.

Acknowledgements and references

The CCP-WSI is funded by EPSRC (EP/M022382/1) [website - www.ccp-wsi.ac.uk]

References:

Ransley, E., … (2019) A blind comparative study of focused wave interactions with a fixed FPSO-like structure (CCP-WSI Blind Test Series 1), *International Journal of Offshore and Polar Engineering*, 29(2): 113-127.

Brown, S. A., Ransley, E. J., Musiedlak, P.-H., Greaves, D., n.d.. Quantifying the Predictive Capability of OpenFOAM 5.0: Focused Wave Impacts with Floating Bodies, *International Journal of Offshore and Polar Engineering*, (in review).

Assessing Free Surface Effects in Tidal Turbine Simulations

Pal Schmitt, Milo Feinberg, Christian Windt and Josh Davidson

Marine Research Group, Marine Laboratory, 12-13 The Strand, Portaferry, Northern Ireland
ORPC Ireland Ltd. Bridge House, Baggot Street Upper Dublin 4, D04 X2P1, Ireland
Department of Electronic Engineering, Centre for Ocean Energy Research, Maynooth University, Maynooth, Co. Kildare, Ireland
Department of Fluid Mechanics, Faculty of Mechanical Engineering, Budapest University of Technology and Economics, Hungary

Figure: ORPC RivGen turbine stationed on Kvichak river, Igiugig Alaska, 2014

Free Surface Effects

Turbines like the ORPC RivGen cross-flow turbine, but also conventional horizontal axis turbines deployed in surface proximity, will be affected by the deformation of the free surface. For industrial design and development, those effects must be taken into account. Fully non-linear volume of fluid methods increase the computational burden significantly compared to single phase solvers, typically used with a slip wall condition at the surface patch.

Compuational model – potentialFreeSurfaceDyMFoamUsrc

potentialFreeSurfaceDyMFoamUsrc is a single phase solver based on pimpleFoam. A special boundary condition based on the linear hydrostatic relationship is used to track surface elevation $\zeta = p/(\rho g)$.
We enhance the original solver with wave and current generation abilities by adding terms to the impulse equation.

$$\frac{\partial(\rho \mathbf{U})}{\partial t} + \nabla\cdot(\rho\mathbf{U}\mathbf{U}) = -\nabla p + \nabla\cdot\mathbf{T} + \rho\mathbf{F}_b + r_w\rho\mathbf{a}_{wm} + r_c\rho\frac{\mathbf{U_t}-\mathbf{U}}{\Delta t} + s\vec{n}_z\rho\mathbf{U}$$

with

- $r_w\rho\mathbf{a}_{wm}$: wave generation
- $r_c\rho\frac{\mathbf{U_t}-\mathbf{U}}{\Delta t}$: current generation. Each cell centre within $r_c = 1$ acceleration input corrects the velocity field $\mathbf{U}$ to target velocity $\mathbf{U_t}$.
- $s\vec{n}_z\rho\mathbf{U}$: numerical beach allowing for a steady current flow in x-direction.

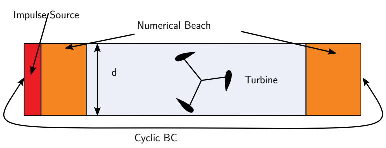

Figure: Computational domain used for the present simulations. The turbine is placed in the middle of the test section. Upstream and downstream a beach dampens waves, but the current imposed by the current generator passes undisturbed.

Simulations are run for a 2D section of the four bladed RivGen turbine, including transverse members of the chassis. Turbine diameter is 1.5m. Computational burden of potentialFreeSurfaceDyMFoamUsrc compared to pimpleFoam with slip wall conditions is negligible.

Acknowledgements

P. Schmitt, M. Feinberg thank the European Union, TAIODE Project, H2020 grant No. 727465.H2020TAOIDE. C. Windt thanks the Science Foundation Ireland, Grant No. 13IA1886. J. Davidson thanks the Water science & Disaster Prevention research area of Budapest University of Technology and Economics (BME FIKP–VÍZ).

Surface deformation and wake

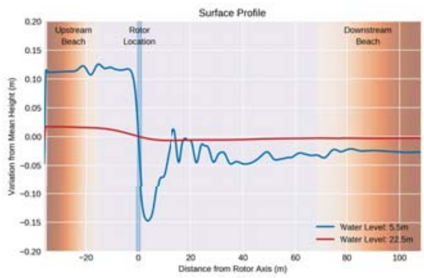

Surface deformation is hardly noticeable for 22.5m water depth, but for 5.5m a bore develops above the turbine.

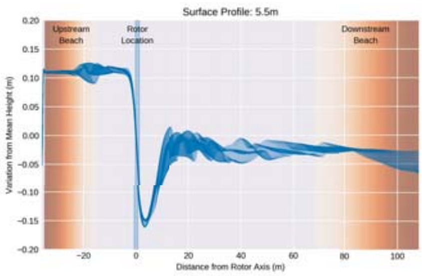

While the bore above the turbine is quasi static, disturbances and instabilities can be observed in the wake downstream of the turbine.

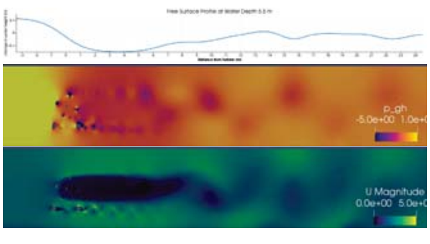

Simulations also allow to investigate the interaction of the wake with the free surface. Close to the turbine, structures with a diameter in the order of magnitude of the blades dominate the flow field. Several diameters downstream the flow is defined by vortices of the scale of the turbine and interacting with the free surface.

Coefficient of power – slip wall bounded vs free surface

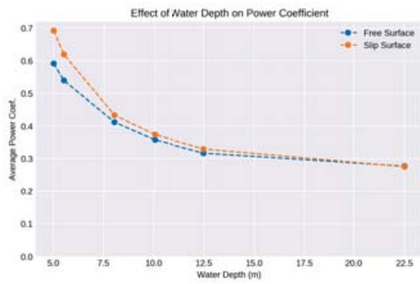

With decreasing water depth, differences between wall bounded and free surface become significant. Though lower than predicted by wall bounded simulations, coefficients of power still reach the Betz limit.

Coefficient of drag – slip wall bounded vs free surface

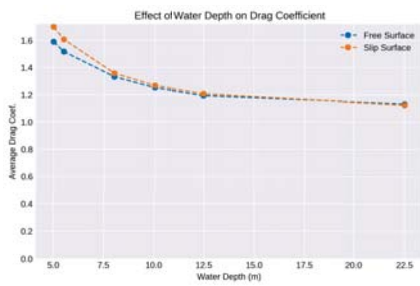

The influence of the water-level on turbine drag is much less than on power capture, but still significant at typical operating conditions.

Conclusions

- Free surface effects must be considered
- Efficiency above the Betz limit is realistic for typical cross flow turbine deployments
- High quality validation data missing for correct Re Number, velocity–depth profile, solidity ...
- potentialFreeSurfaceDyMFoamUsrc might be an efficient option for further hydrodynamic problems, evaluation ongoing...

Learning-Based Robust Control for Offshore Wave Energy Converters

Mr. Shuo Shi & Prof. Ron J. Patton

University of Hull, S.shi@2016.hull.ac.uk, R.J.Patton@hull.ac.uk

Background

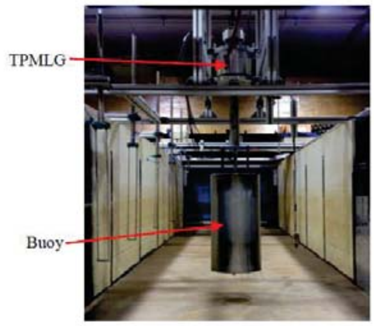

PAWEC installed in the University of Hull.

Wave energy has potential to contribute up to 2.1 TW power worldwide. A prime goal is to reduce the high Levelized Cost of Energy (LCoE) of wave power in order to reach commercial Wave Energy Converter (WEC) applications.

Optimal control of WEC requires:

- Wave Excitation Force (WEF) Estimation
- Wave and WEF prediction
- Robust & Optimal controller for WEC

★ Research Aim ★

Propose robust & optimal control strategy for WEC to maximizing energy conversion under constraints

Work Overview

A. Short-term Wave Forecasting for Optimal Control of WECs

➢ **Problem Description**

WEF or wave elevation prediction is required for WEC power efficiency maximization control due to inherent non-causality of required power take-off (PTO)force.

➢ **Wave Forecasting Strategy**

The Gaussian Process (GP) model for short-term wave forecasting shows better or comparative performance with Neural Network (NN) and Autoregressive (AR) modelling methods.

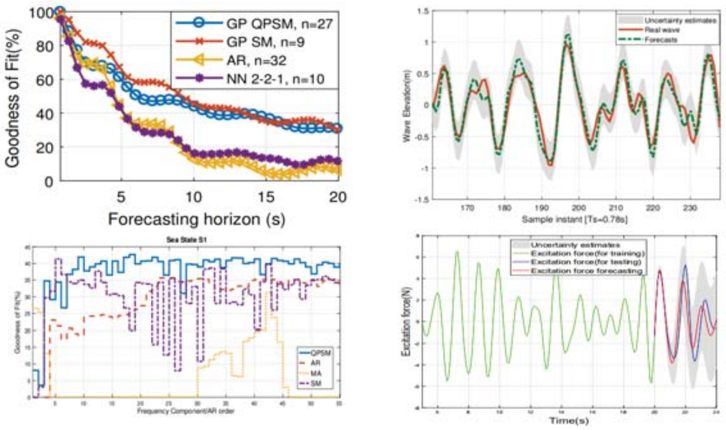

B. Robust Data-driven Estimation of Wave Excitation Force

➢ **Method Description**

Data-driven approach to estimate wave excitation force (WEF), using robust Bayesian filter described by non-parametric Gaussian process (GP) models. A first principle model in a probabilistic framework is more robust than calculating estimates of a parametric function representation. the means and covariances of joint probabilities can be directly computed based on analytic moment matching.

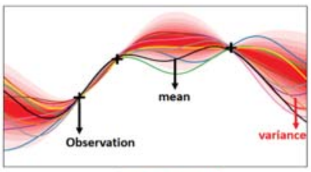

the GP model

➢ **Results**

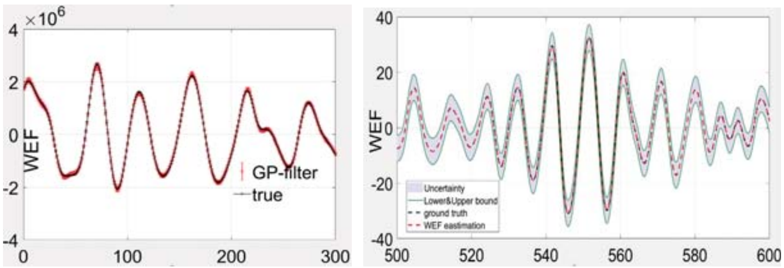

WEF estimation results

C. WECCCOMP – WEC CONTROL COMPETITION

➢ **WECCCOMP Description** *

Wave Energy Control Competition is organized by COER at Maynooth University in cooperation with Sandia National Laboratories, NREL in USA, Centre for Marine and Renewable Energy (MaREI), and Aalborg University. Our data-efficient learning approach ranks top 3.

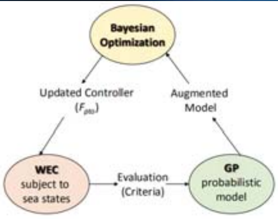

Block diagram of the Bayesian learning reactive control

➢ **Control Strategy**

Bayesian Optimization algorithm is adopted to learn the optimal coefficients of the causal controller subject to physical constraints.

➢ **Results**

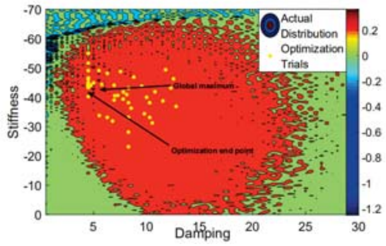

Regular waves

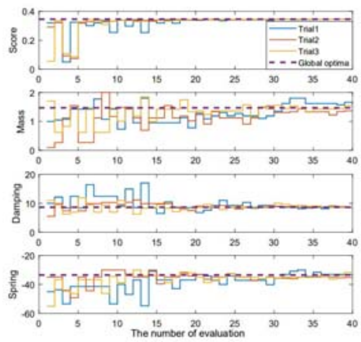

Irregular waves

Future Work

❖ Our entry in WECCCOMP competition is being extended to a WEC array problem using parallel Bayesian Optimization.

❖ Gaussian Process Model-based Predictive Control (GP-MPC) will be developed for WECs. By exploiting Pontryagin's Maximum Principle our algorithm can deal with state and control constraints in a robust way.

Centre for Ocean Energy Research · Sandia National Laboratories · NREL National Renewable Energy Laboratory · Aalborg University Denmark · MaREI Centre for Marine and Renewable Energy · University of Hull

One-fluid formulation for floating offshore renewable energy devices

Liang Yang (Liang.Yang@cranfield.ac.uk), Dimitris Stagonas (D.Stagonas@cranfield.ac.uk),

- One-fluid framework for multiphase fluid, rigid structure, large deformable structure, articulated structure interaction
- Equal computational costs as high fidelity multiphase fluid solver
- Applications: Floating ORE Platforms
- Extension to 3D is our on-going work

High Fidelity Fluid Solver: Arbitrary phases with Level Sets

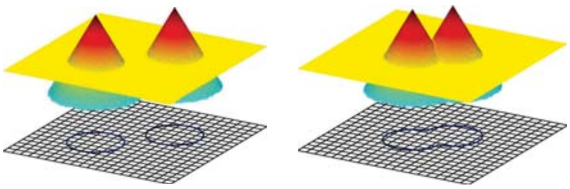

Fig. 1 Level Set representation of an interface.

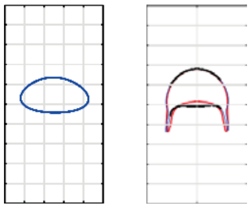

Fig. 2 Rising bubble with different surface tension.

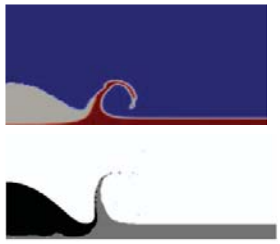

Fig. 3 Liquid dropping on a thin layer, Three phases.

High Fidelity Fluid-Structure Solver: Arbitrary deformable solids with contacts

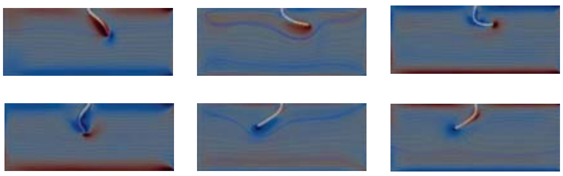

Fig. 4 Time evolution of a incompressible flexible membrane under pulsatile flow.

Fig. 5 Time evolution of the interaction between a wave hitting an elastic wall.

High Fidelity Fluid-Structure Solver: Arbitrary articulated rigid structure

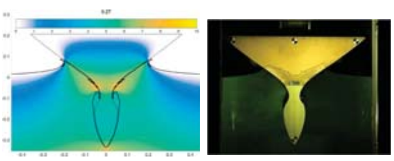

Fig. 5 Pressure distribution and free surface for a water impact problem.

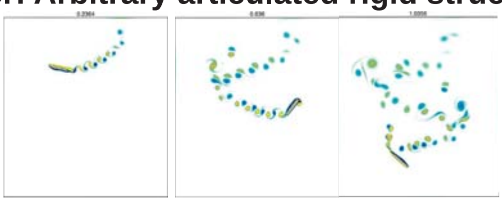

Fig. 6 Fluttering plate in a viscous fluid.

Fig. 7 Double pendulum motion in viscous fluid.

Numerical Wave Tank

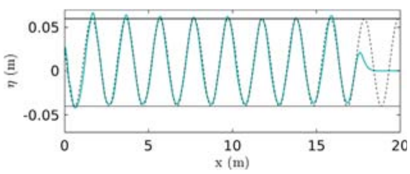

Fig. 8 Regular wave generation and absorption.

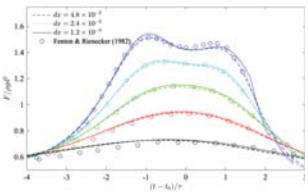

Fig. 9 Solitary wave generation.

Fig. 10 Solitary wave run-up and experiment.

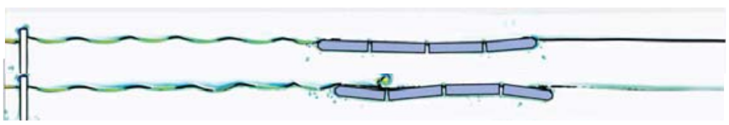

Fig.11 Dynamic response of attenuator type of wave energy converters.

Bayesian Ecosystem and Natural Capital Models to Understand the Effect of Offshore Renewables on the Marine System

Neda Trifonova (Research fellow, UoA) and Beth Scott (Professor, UoA)

1. Introduction

- The UK is at the forefront of the development, adoption and export of offshore renewable energy (ORE) technologies.
- Climate change is a major concern, leading to predictions of a global temperature rise of 3–5 °C within 50 years.
- Understanding how usage of spatial habitat of highly mobile marine species may change with climate change and large-scale energy extraction devices is essential for sustainable management of their populations.
- Computational ecosystem models to provide indications of how the ecosystem is likely to change.
- Model parameterization to explore a range of scenarios to investigate optimal locations and design of ORE technologies.
- Natural capital models need to be developed to forecast the ecological and socio-economic benefits and trade-offs that will occur with the operation of ORE technologies and future climate change, which is vital for the sustainable management of all uses of our marine ecosystems.

2. Bayesian Networks

Bayesian networks (BNs) are models that graphically and probabilistically represent relationships among variables.

- BNs can capture nonlinear, dynamic and arbitrary combinatorial relationships.
- BNs efficiently integrate variables presented at different scales.
- Empirical data can be combined with existing knowledge.
- BNs integrate the uncertainty associated with species dynamics due to the action of multiple driving factors and can be used for environmental decision making.
- BNs can use different 'currencies': ecological, economic (natural) and social capital.

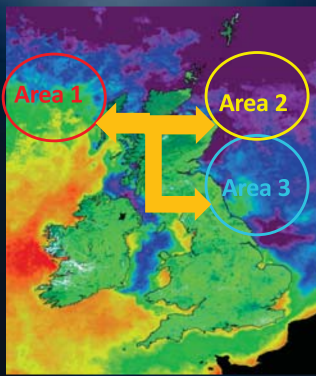

Area 1

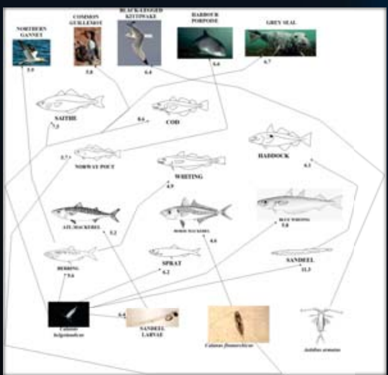

Area 2

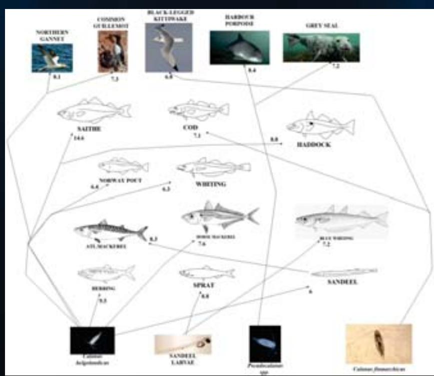

Area 3

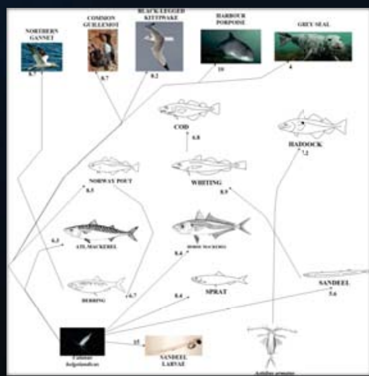

3. Bayesian Ecosystem and Natural Capital Models and ORE Supergen

- Develop and validate Bayesian ecosystem models to support the confident prediction of the environmental impact of ORE technologies.
- Opportunities to work with government establishments to design coastal management plans that facilitate sustainable use of the environment, benefiting locals and the global community.

Define the Area(s) using Site Selection: Real and Virtual sites → Research to Test and Validate Modelling Assumptions and Parameters → Identify the Scale and Significance of Population Level Impacts → Test Models with different Currencies- Natural/Social Capital Changes → Identify Opportunities for Transfer of Research between Sectors

Computational Fluid Dynamics Models + Finite-Volume Community Ocean Model + European Regional Seas Ecosystem Model → Whole System Approach: Bayesian Ecosystem Model

\+

Test Deployment Scenarios with Energy System Models (ESME) → Technology Innovation: Investigate How Devices Need to Change and Innovate → Assessment Metrics: Gross Value Added and Levelized Cost of Energy to Investigate How Coastal Communities will Benefit → Life-Cycle Cost Assessment to Determine Global Warming Potential, Energy Return on Investment and Energy Payback Time

Key References:

1) Hooper, T., Beaumont, N. and Hattam, C., 2017. The implications of energy systems for ecosystem services: a detailed case study of offshore wind. Renewable and Sustainable Energy Reviews, 70, 230- 241.
2) De Dominicis, M., Wolf, J. and O'Hara Murray, R., 2018. Comparative effects of climate change and tidal stream energy extraction in a shelf sea. Journal of Geophysical Research: Oceans, 123(7), 5041-5067.
3) Sadykova, D., Scott, B.E., De Dominicis, M., Wakelin, S.L., Sadykov, A. and Wolf, J., 2017. Bayesian joint models with INLA exploring marine mobile predator–prey and competitor species habitat overlap. Ecology and evolution, 7(14),5212-5226.

A Risk Assessment Framework for Offshore Wind Turbines

David Wilkie (david.wilkie.15@ucl.ac.uk) Dr Carmine Galasso (c.galasso@ucl.ac.uk)
Dr Phillippe Duffour (p.duffour@ucl.ac.uk)
UCL

1) Motivation

The design and assessment of offshore wind turbines (OWTs) is currently based on **deterministic, prescriptive approaches**. However, there are uncertainties associated with structural assessment through

- Stochastic environmental loading as a result of wind and waves.
- Structural capacity: materials, geometry and models.

Neglecting these uncertainties may lead to over-conservative design or unsafe designs that can fail catastrophically. This project **proposes a risk-based approach for the assessment of offshore wind farms (OWFs)**.

2) Assessment cases

OWT structures are currently assessed against three performance objectives (or limit states) – however **not all drive failure of the structure** [1] and do not need included within a risk assessment. The design cases considered in this work include:

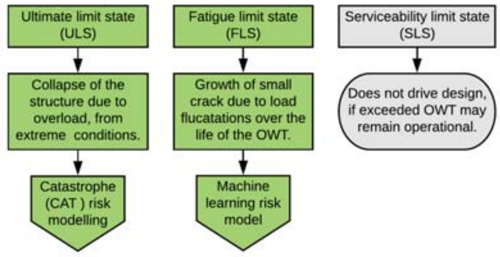

3) Ultimate limit state

Extreme environmental conditions
Data measured at two real OWF sites.

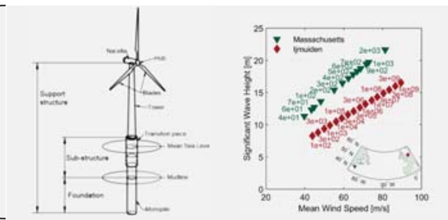

Component limit states
For tower, monopile, blades and transition piece.

Structural analysis
Dynamic time-history analysis in FAST software package.

Fragility curves [2]:

- Tower, lognormal fragility curve
- Blades – empirical fragility curve (lognormal was found to provide a poor fit)
- Sub-structure, no fragility curve required because component did not fail.

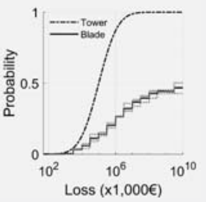

Component fragility
Incremental wind-wave analysis and fragility fit using maximum likelihood estimation.

Component annual failure rate
For all structural components.

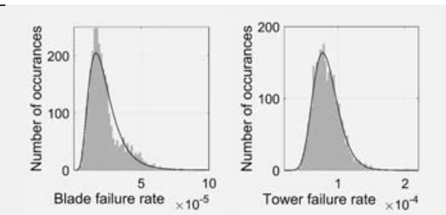

4) Fatigue limit state

Operational environmental conditions
Data measured at North Sea OWF site.

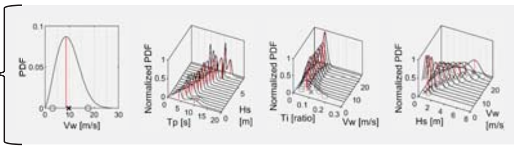

Structural analysis
Dynamic time-history analysis in the FAST software package.

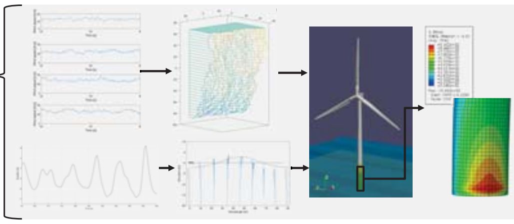

Machine learning
Gaussian process regression meta-model for structural analysis.

Uncertainty in fatigue life
SN curve parameters modelled as random variables.

Fatigue life estimated using empirically measured parameters. Causing large uncertainty in the relationship between number of cycles to failure and the stress range.

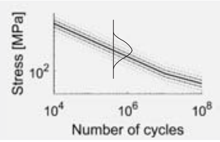

Component annual failure rate
For the monopile at the seabed.

Large scatter in the failure of OWT due to the FLS observed [3]:

- Gaussian process regression provided a computationally efficient meta-model
- Enables Monte Carlo sampling of uncertain parameters

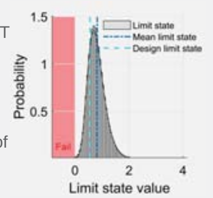

5) Loss

Loss is evaluated for the OWT structure, also considering the most expensive 9 pieces of electrical / mechanical equipment.

Source of cost data	Component	Major replacement [€]	Failure rate [/turbine/year]
Carroll [4]	Gearbox	230,000	0.154
	Hub	95,000	0.001
	Transformer	70,000	0.001
	Generator	60,000	0.095
	Circuit breaker	14,000	0.002
	Power supply	13,000	0.005
	Pitch system	14,000	0.001
	Yaw system	13,000	0.001
	Controller	13,000	0.001
	Blades (x3)	270,000	Wilkie & Galasso [5]
Parametric equations	Tower	770,000	Wilkie & Galasso [5]
	Monopile	2,380,000	Wilkie & Galasso [3]
	Total cost	3,942,000	

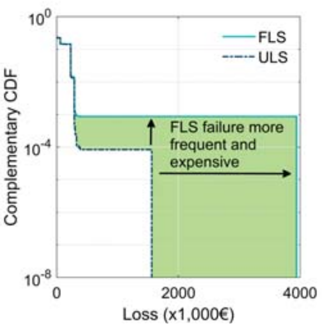

6) Conclusion

- **Largest annual losses are from FLS**, because failure has a higher likelihood and involves the sub-structure, as well as the tower – indicated below where losses from ULS and FLS are compared.
- Failure in **ULS are larger if severe hurricane** conditions expected, such as at proposed wind farms on the East coast of the United States [2].

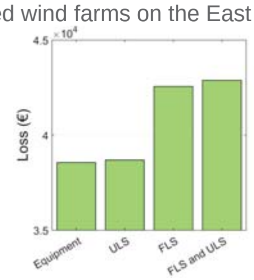

EPICentre

References

[1] Vorpahl F et al. Offshore wind turbine environment, loads, simulation, and design. Wiley Interdiscip Rev Energy Environ 2013;2:548–70. doi:10.1002/wene.52. [2] Wilkie D at al. Site-specific ultimate limit state fragility of offshore wind turbines on monopile substructures. Eng Struct [201X]. [3] Wilkie D et al. Fatigue Reliability of Offshore Wind Turbines using Gaussian Processes. ICASP2019 [2019]. [4] Carroll J et al. Failure rate, repair time and unscheduled O&M cost analysis of offshore wind turbines. Wind Energy 2016;19:1107–19. doi:10.1002/we.1887. [5] Wilkie D et al. Towards structurally resilient offshore wind farms. Renewable Energy [201X].